THE UNIVERSITY OF MICHIGAN

COLLEGE OF ENGINEERING

Department of Nuclear Engineering
Laboratory for Fluid Flow and Heat Transport Phenomena

Technical Report No. 4

COMPREHENSIVE CAVITATION DAMAGE DATA FOR WATER, MERCURY, AND LEAD-BISMUTH ALLOY INCLUDING CORRELATIONS WITH MATERIAL AND FLUID PROPERTIES

R. Garcia
F. G. Hammitt
R. E. Nystrom

Financial Support Provided by:

National Science Foundation
(Grant G-22529)

administered through:

OFFICE OF RESEARCH ADMINISTRATION ANN ARBOR

May, 1966

ACKNOWLEDGMENTS

Financial support for this investigation was provided by a grant from the National Science Foundation. Mechanical properties data supplied by Pratt & Whitney Aircraft (CANEL) and The University of Michigan Department of Chemical & Metallurgical Engineering is also gratefully acknowledged.

Special thanks are also due Dr. Clarence A. Siebert, Dr. M. John Robinson, Mr. Richard L. Crandall, and Mr. Allen R. Schaedel, University of Michigan, and Mr. Henry Leeper and Mr. Glenn Wood, Pratt & Whitney Aircraft (CANEL), for many helpful suggestions and continuing interest in this project.

ABSTRACT

Ultrasonic-induced cavitation studies have been conducted in lead-bismuth alloy at 500°F and 1500°F, in mercury at 70°F and 500°F, and in water at 70°F for a wide variety of materials, including refractory alloys, steels, brasses, copper, nickel, plastics, etc. Comprehensive computer correlations of the cavitation damage data with applicable mechanical and fluid properties have been carried out. The major conclusions of the study are:

1) The tantalum-base alloys were the most cavitation resistant in all the tests except in mercury at 70°F, where the stainless steels were the most resistant.
2) All materials tested in lead-bismuth at 500°F and 1500°F, and all materials tested in mercury at 70°F and 500°F sustained greater damage at the higher temperature with the exception of carbon steel.
3) Corrosion effects in those regions where cavitation was absent were negligible in this investigation.
4) Damage rates in mercury were 3 to 20 times greater than in water, depending upon the material. Hence, clearly no correlating equation which considers only the mechanical properties of the material can apply for both fluids.

5) There is no single material mechanical property which can be used to correlate the damage, even if coupling parameters to account for fluid property changes are included in the correlation.

6) In general, the best correlations include energy-type mechanical properties, strength-type properties, and fluid coupling parameters.

7) No relatively simple single correlating equation applies well to all the data. This may indicate the insufficiency of the statically-determined mechanical and fluid properties for the correlation of cavitation damage which is known to be a highly transient process.

TABLE OF CONTENTS

LIST OF FIGURES

Figure Page

LIST OF TABLES

CHAPTER I

INTRODUCTION

A. Importance of Cavitation Studies

Cavitation can be described as a hydrodynamic phenomenon which relates to the formation and collapse of vapor bubbles in a liquid under essentially adiabatic conditions. However, according to present theory the cavitation damage process is very closely related to damage from droplet or particle impingement or conventional erosion.* Thus the cavitation damage data is also to some extent applicable to the resistance of the same materials to these other forms of attack, so that the fields of droplet erosion in wet vapor streams (as in turbines or other two-phase flow passages), rain erosion of high-speed aircraft, micrometeorite bombardment of space vehicles, etc., are involved.

The successful pumping and handling of high-temperature liquid metals, wherein cavitation itself is a problem, is of considerable importance to the space program, particularly SNAP liquid-metal Rankine cycle power-conversion equipment. As has been recently demonstrated, damaging cavitation attack can occur in bearings,[2] close-clearance passages,[3] etc., as well as pumps.[4,5]

---

*Reference (1) includes many papers on the relations between these various forms of attack, including one by one of the present authors.

B. Accelerated Cavitation Studies

In a prototype system, the damage due to cavitation appears usually only after fairly lengthy operation under design conditions. Hence, a systematic study of this type, covering a variety of materials and plant conditions, will involve considerable cost and time. An alternate approach, sacrificing direct applicability to some extent in the interests of economy, is to accelerate the cavitation losses by employing any one of several laboratory techniques which have been developed for this purpose. For the present investigation we have followed this course using a vibratory cavitation device. In our own laboratory we also employ a flowing venturi system.[6] While the venturi is reasonably similar to actual flowing systems, damage occurs only rather slowly. Although it is our eventual purpose to compare results from the vibratory and venturi systems, this aspect of our overall program is not covered in the present paper.

In addition to the cavitation testing program, it is essential to determine the applicable mechanical properties of the materials tested at the test temperatures so that a correlation between resistance to this form of two-phase attack and some combination of the mechanical properties can be obtained, if, indeed, such a general correlation with the statically-determined mechanical properties exists. Applicable mechanical properties include ultimate tensile strength, yield strength, hardness, strain energy to failure, elongation, reduction in area, impact resistance, etc. If several fluids are involved, the correlation would be expected to include terms which are functions of applicable

fluid properties, such as density, surface tension, net positive suction head, bulk modulus, kinematic viscosity, acoustic impedance ratio, etc.

C. High-Temperature Ultrasonic Cavitation Vibratory Facility

The University of Michigan high-temperature ultrasonic cavitation vibratory facility has been described elsewhere.[6,7] However, the major features of the facility will be reviewed here. Figure 1 is a schematic showing the arrangement of the audio oscillator, power amplifier, transducer-horn assembly, test specimen, oscilloscope, frequency counter, high-temperature furnace and cavitation vessel, and accelerometer. For studies at elevated temperatures the transducer-horn assembly is attached to the special cavitation vessel which is filled with the appropriate fluid. The accelerometer, oscilloscope, and frequency counter are used to monitor the amplitude and frequency of vibration of the horn tip during the tests.[8] Argon cover gas for the fluid is used under suitable pressure to maintain uniform suppression pressure for all tests.

The cavitation facility has been operated at fluid temperatures in excess of 1500°F at a nominal frequency of 20 Kc./sec. and double amplitude of 2 mils. It is capable of operation with a variety of fluids.

D. Present Investigation

To date cavitation-erosion data have been obtained in lead-bismuth alloy (70 per cent lead - 30 per cent bismuth) at 500°F and

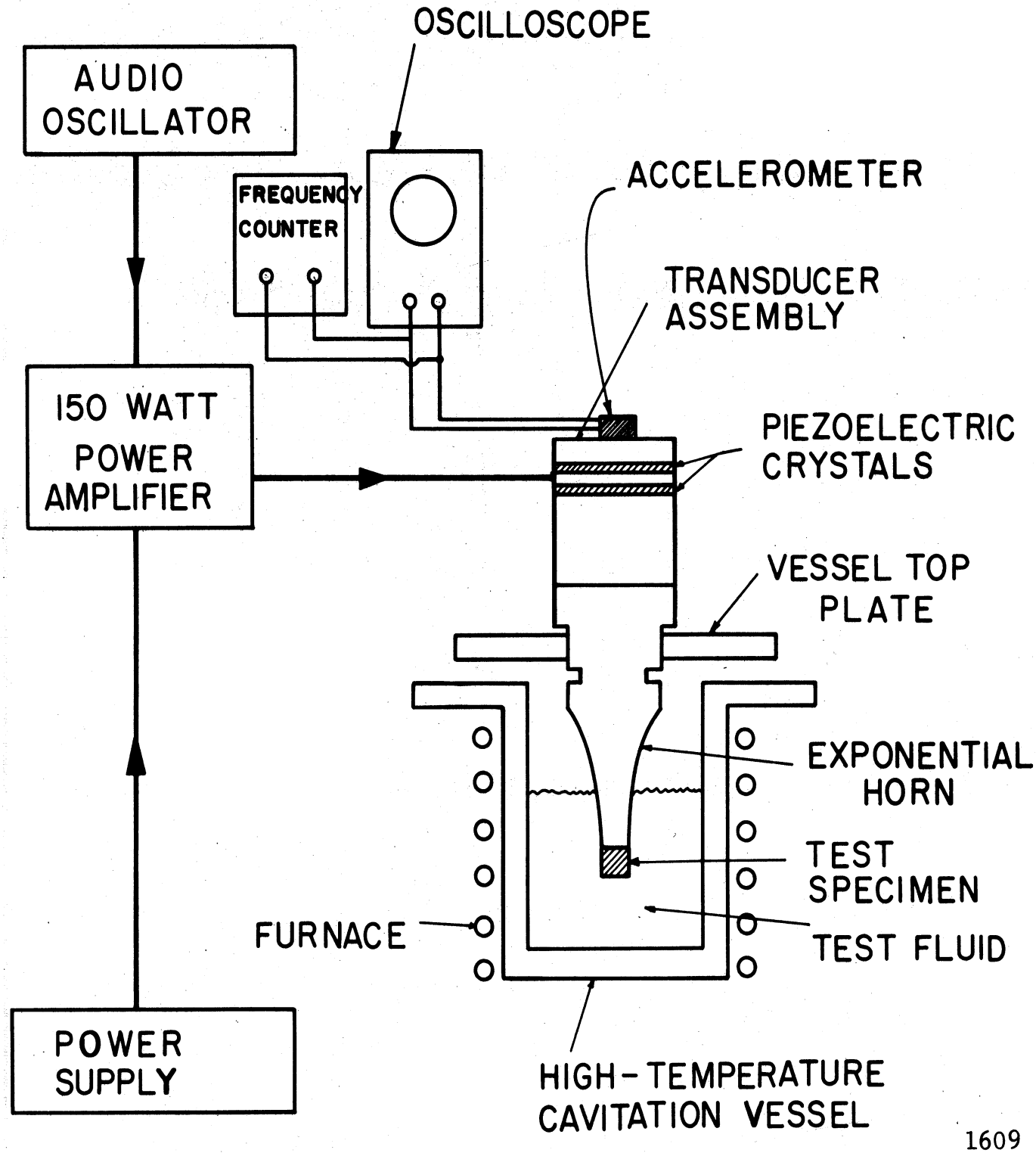

Figure 1. Block Diagram of the High-Temperature Ultrasonic Vibratory Facility

1500°F,[9,10,11,12] in mercury at 70°F and 500°F,[13,14] and in water at 70°F[13] for a variety of materials, utilizing this facility. Although somewhat related data has also been obtained in our venturi facility, this paper is concerned exclusively with the studies conducted in the ultrasonic vibratory facility. Table 1 summarizes the specimen material-fluid-temperature combinations which were studied in this investigation, and the meaning of the various symbols used in the description of these materials.

Table 1--Specimen Material-Fluid-Temperature Combinations Investigated

Material	Fluid			
	Water 70°F	Mercury 70°F	Mercury 500°F	Pb-Bi 500°F & 1500°F
1100-0 Al (U-M)	X	...	...	...
2024-T351 Al (U-M)	X	...	...	...
6061-T651 Al (U-M)	X	...	...	...
304 Stainless Steel (U-M)	X	X	X	X
316 Stainless Steel (U-M)	X	X	X	X
Hot-Rolled Carbon Steel (U-M)	X	X	X	...
T-111 (Ta-8W-2Hf) (P & W)	X	X	X	X
T-222 (Ta-9.5W-2.5Hf-.05C) (P & W)	X	X	...	...
T-222(A) (P & W)	...	...	X	X
Mo-1/2Ti (P & W)	X	X	X	X
Cb-1Zr (P & W)	X	X	X	X
Cb-1Zr(A) (P & W)	X	X	X	X
Plexiglas (U-M)	X	X	...	...
Cu(60% cold-worked) (U-M)	X	...	...	...
Cu(900°F anneal, 1 hour) (U-M)	X	...	...	...
Cu(1500°F anneal, 1 hour) (U-M)	X	...	...	...
Cu-Zn(60% cold-worked) (U-M)	X	...	...	...
Cu-Zn(850°F anneal, 1 hour)(U-M)	X	...	...	...
Cu-Zn(1400°F anneal, 1 hour)(U-M)	X	...	...	...
Cu-Ni(60% cold-worked) (U-M)	X	...	...	...
Cu-Ni(1300°F anneal, 1 hour)(U-M)	X	...	...	...
Cu-Ni(1800°F anneal, 1 hour)(U-M)	X	...	...	...
Ni(75% cold-worked) (U-M)	X	...	...	...
Ni(1100°F anneal, 1 hour)(U-M)	X	...	...	...
Ni(1600°F anneal, 1 hour)(U-M)	X	...	...	...

Notes:

1) "X" indicates test conducted for this specimen material-fluid-temperature combination.
2) The notations (U-M) and (P & W) following the specimen materials indicate the source of the material, namely, The University of Michigan and Pratt & Whitney Aircraft (CANEL), respectively; whereas the notation (A) denotes an annealed condition of the material.

CHAPTER II

EXPERIMENTAL PROCEDURE

A. Test Specimens

Standard test specimens (Figure 2) were machined from bar stock for all materials tested except Plexiglas, Cu, Cu-Zn, Cu-Ni, and Ni. The required height dimensions "A" and "B" (Figure 2) are varied for each material to provide a standard specimen weight (9.4 $\pm$ 0.1 g.) which is necessary for resonance. For stainless steel, "A" and "B" are 0.250 in. and 0.625 in., respectively.

Due to its very low density and brittle nature, it was impractical to utilize standard test specimens of Plexiglas. The low density required an unfeasibly large height, while the brittleness of the material made it impossible to attach a specimen to the ultrasonic horn with adequate firmness without damage to the thread. A tight attachment is necessary so that the ultrasonic energy is efficiently transmitted across the interface. Hence, a design consisting of a Plexiglas test specimen with internal threads and a separate stainless steel mounting stud, which provides adequate mass, was adopted and proved satisfactory (Figure 3).

It was desired to test the identical heat-treats of Cu, Cu-Zn, Cu-Ni, and Ni in the vibratory facility that had been previously tested

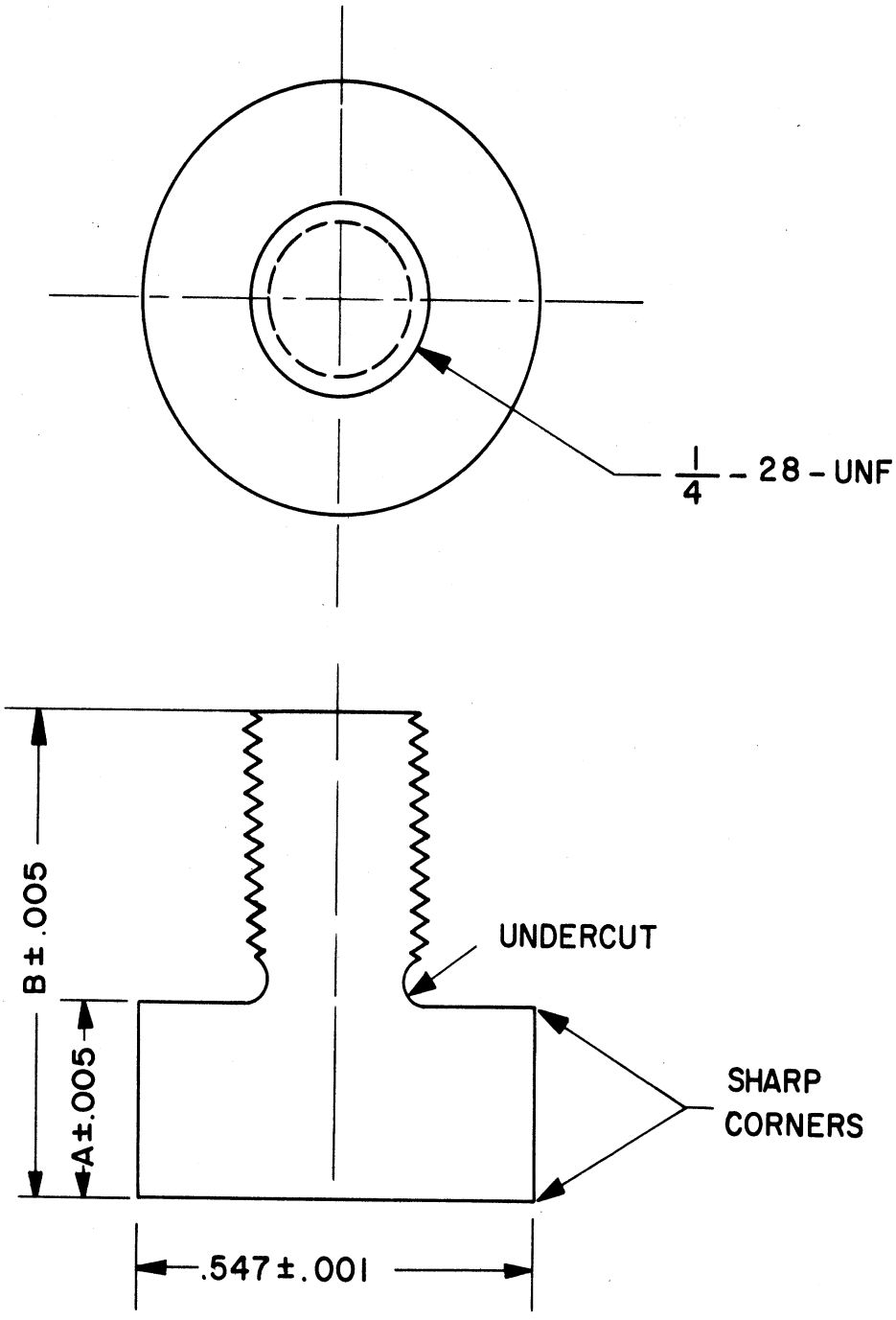

NOTE :
DIMENSIONS "A" & "B"
VARY WITH SPECIMEN MATERIAL

1455

Figure 2. Standard Cavitation Test Specimen

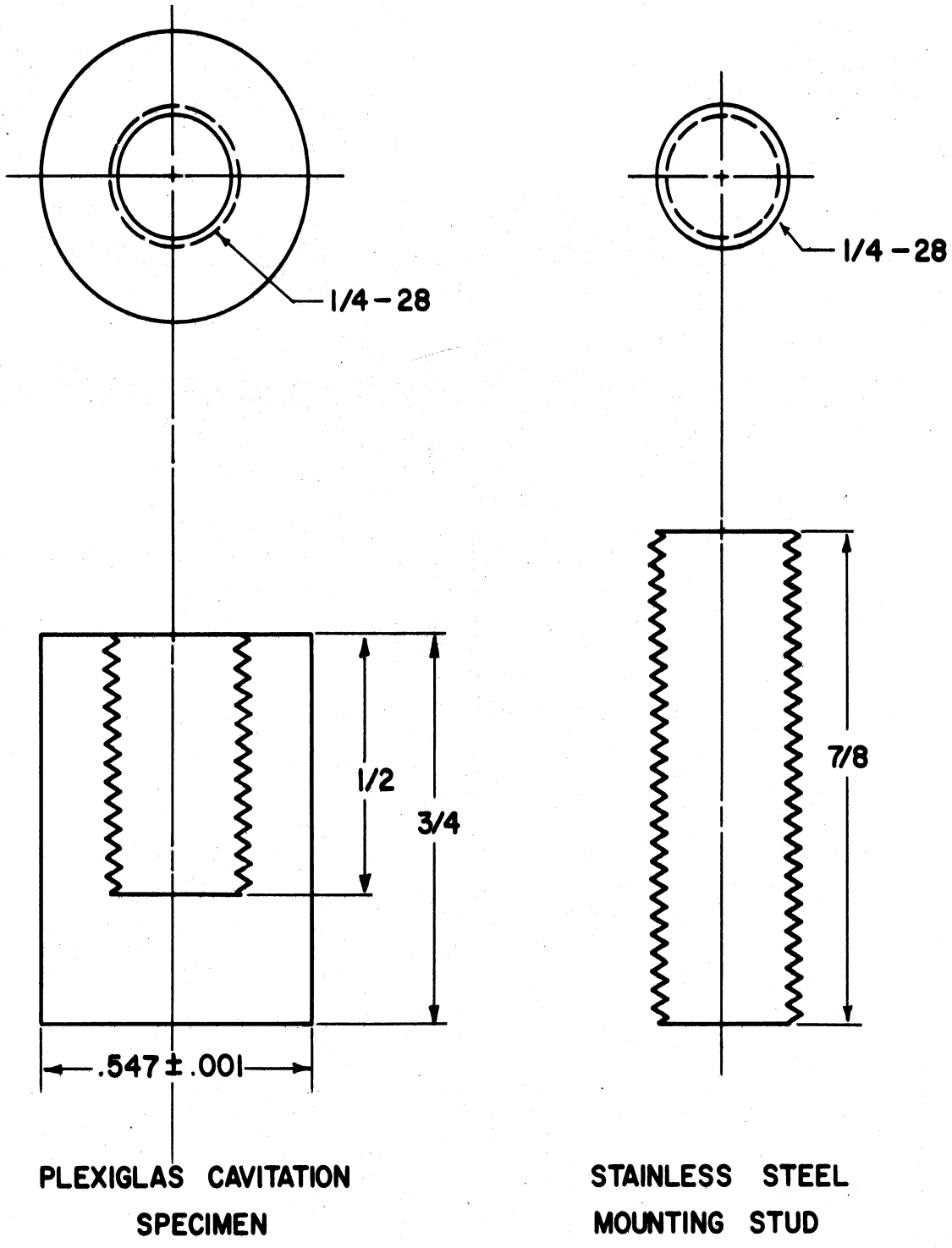

Figure 3. Special Plexiglas Cavitation Specimen and Mounting Stud

in the venturi loop facility, so that a very direct comparison of results would be possible. Since these materials had been procured only in 1/16 in. sheet stock for the venturi specimens, it was necessary to design a special specimen for the vibratory test, consisting of an adaptor of a suitable material (similar in shape to the standard specimen of Figure 2) and a disc of the desired material. It was necessary, then, to provide a suitably firm attachment between disc and adaptor. The adaptors were fabricated from brass bar stock, and the disc of the desired material was attached using soft solder, taking care not to heat the test material to a temperature which would significantly change its properties. The bond provided by various epoxies and cements had previously been found inadequate. While the acoustic impedance of the soft solder is similar to that of both the brass adaptor and disc materials, this was not the case for the epoxies and cements. The design adopted results in the desired specimen weight.

B. Test Conditions

Initially, each of the specimens was weighed on a precision electronic balance to an accuracy of 0.01 mg., and then attached to the tip of the stainless steel exponential horn, whereupon the unit was assembled.

The tests in lead-bismuth alloy at 500°F and 1500°F and in mercury at 70°F and 500°F were conducted in the 316 stainless steel cavitation vessel previously mentioned. The investigations in water at 70°F were conducted in a Plexiglas cavitation vessel whose dimensions were

identical to those of the 316 stainless steel container. The Plexiglas vessel permits visual observation of the bubble cloud and the condition of the specimen surface during a test.

At elevated temperatures the test fluid was maintained at the required temperature by a suitable controller, which allowed temperature variations of less than 5°F.

The specimens were oscillated at 20 Kc./sec. $\pm$ .002 Kc./sec. with the exception of the 1500°F tests where the resonant frequency was 18 Kc./sec. $\pm$ .002 Kc./sec. The submergence of the horn tip was held constant at 1-1/2 $\pm$ 1/8 inches in all fluids, while the double amplitude at the specimen was maintained at 2 mils $\pm$ 0.1 mils for all the tests, as determined by a precision accelerometer.[8]

The argon cover gas pressure was ajusted to maintain constant static pressure above vapor pressure (suppression pressure) for all fluids at the specimen face. The lead-bismuth tests at 500°F and 1500°F and the mercury tests at 70°F were conducted at a slight overpressure (0.5 psig) to prevent inward leakage of oxygen, and the corresponding suppression pressure was used for the remainder of the tests. The mercury tests at 500°F then required an argon pressure of 2.4 psig, and the water tests at 70°F an argon pressure of 1.1 psig because of the different densities and vapor pressures of these fluids. While a constant suppression head, rather than pressure, may have been desirable, the pressure capabilities of the equipment were not adequate to allow this course to be pursued.

Total test duration varied for the different materials and was always sufficient to obtain a good determination of damage rate which, neglecting the very early portion of the test, was found to be essentially linear within the total accumulated damage obtained. Test duration was thus a function of the fluid and fluid temperature, and as shown in the figures differed widely for different materials. The tests were terminated when the complete face of the specimen was damaged, and an approximately uniform rate of damage established. Frequent inspections and weighings were made during the tests to monitor the condition of the specimen surface and establish the rate of weight loss. In the mercury tests prior to weighing, it was necessary to remove any excess mercury adhering to the surface by heating in a vacuum furnace, thus eliminating oxidation of the specimen. In the lead-bismuth tests all transfers of the specimens to and from the high-temperature cavitation vessel were made at a fluid temperature of 500°F. At each examination excess lead-bismuth adhering to the test specimen was removed by quickly heating with a propane torch to a temperature just above the melting point of the lead-bismuth alloy ($\sim$350°F). The excess fluid was then separated from the test specimen by a very brief blast of compressed air. The process was rapid enough so that only negligible oxidation occurred.

Heating time from 500°F to 1500°F for the lead-bismuth tests is approximately 1-1/2 hours. Cooling time from 1500°F to 500°F is approximately five hours.

Since the piezoelectric crystals must be maintained at a temperature below 150°F (Curie point), the top plate of the cavitation vessel is water cooled. A fan provided additional cooling.

CHAPTER III

EXPERIMENTAL RESULTS

A. General

The cavitation damage data is shown as accumulative mean depth of penetration (MDP) versus test duration. We believe the mean depth of penetration, computed assuming that the weight loss is smeared uniformly over the cavitated specimen surface, is more physically meaningful than weight loss, since it is generally the total penetration of a particular component by cavitation erosion that would render it unfit for service. Of course, neither weight loss nor MDP is sensitive to damage distribution and form, i.e., damage may vary from isolated deep pits to relatively uniform wear, depending on material-fluid combination. Obviously, as a "figure of merit" MDP at least takes into account the large variation in density that may occur within a set of test materials.

B. Lead-Bismuth Alloy at 500°F (Reference [12])

Figure 4 shows accumulative MDP versus test duration for the seven materials tested in lead-bismuth alloy at 500°F. The slopes of these curves, representing the average damage rate in mils/hr. are listed in Table 2 along with rates of weight loss. This data from Ref. (12) is included here for completeness.

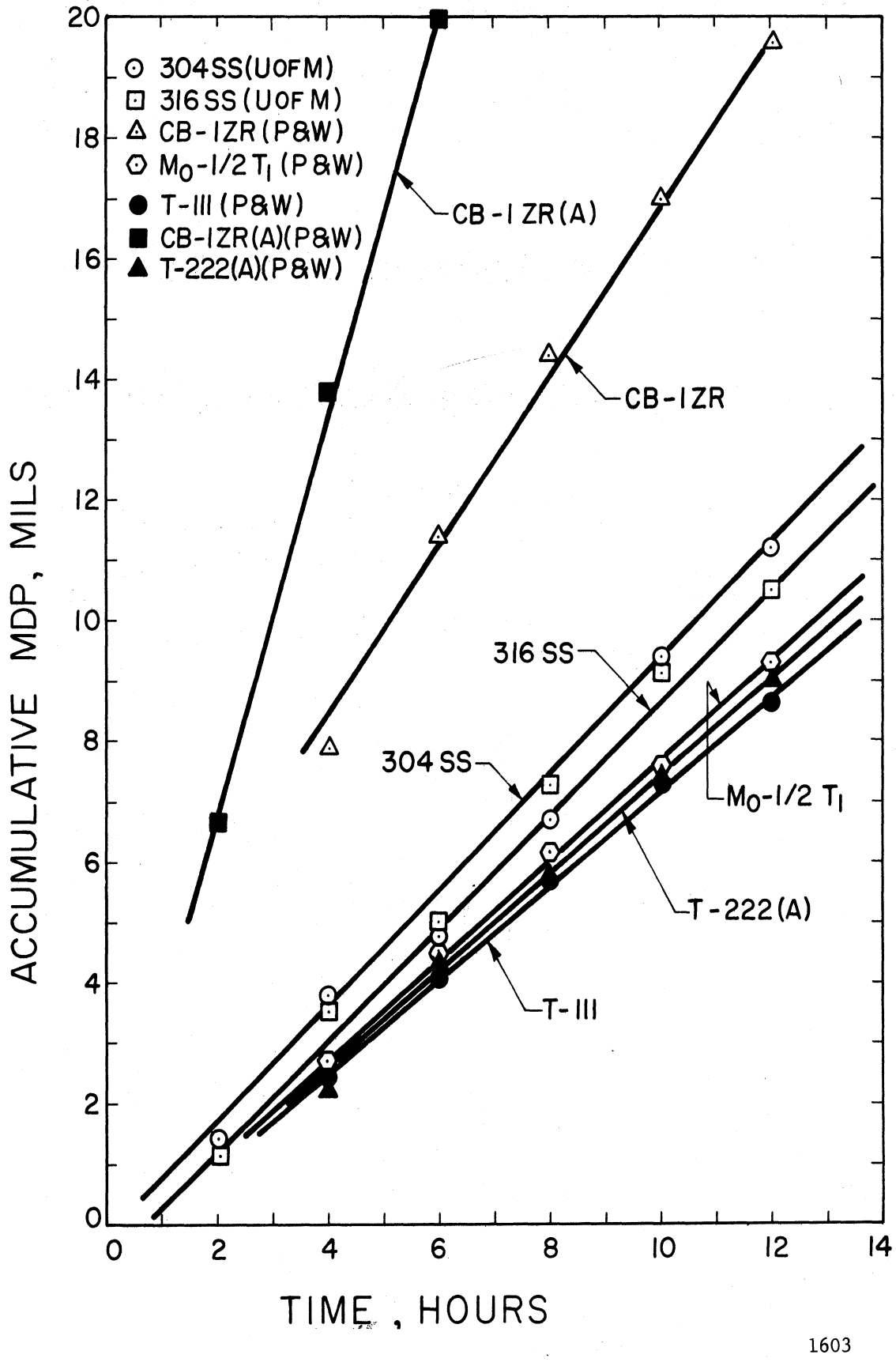

Figure 4. Effect of Cavitation Test Duration on MDP at 500°F in Lead-Bismuth Alloy

Table 2--Summary of Cavitation Results in Lead-Bismuth at 500°F

Material	Avg. Wt. Loss Rate	Average MDP Rate
T-111 (P & W)	49.1 mg./hr.	.72 mils/hr.
T-222(A) (P & W)	51.6	.76
Mo-1/2Ti (P & W)	30.7	.78
316 SS (U-M)	26.6	.88
304 SS (U-M)	28.2	.93
Cb-1Zr (P & W)	55.1	1.63
Cb-1Zr(A) (P & W)	119.5	3.54

On the basis of MDP the alloy T-111 (P & W) exhibited the greatest resistance to cavitation in this experiment, followed in order by T-222(A) (P & W), Mo-1/2Ti (P & W), 304 stainless steel (U-M), and 316 stainless steel (U-M). Cb-1Zr (P & W) and the Cb-1Zr(A) (P & W) were considerably less resistant than the others so that the Cb-1Zr(A) test was concluded after only eight hours of testing, versus twelve hours for the others. It is clear from Figure 4 that the rate of erosion for each individual material was approximately constant. These tests cover a range up to ~12 mils MDP, so that within this range approximately constant rates can be expected. Note that at 500°F the stainless steels fared almost as well as the refractory alloys T-111, T-222(A), and Mo-1/2Ti.

Figure 5 shows photographs of the test specimens before exposure and at the conclusion of the cavitation experiment.

Detailed examination of the 303 stainless steel exponential horn, the 316 stainless steel container vessel, and the sides of the various test specimens, all of which are <u>not</u> subject to cavitation, but <u>are</u> submerged in the test fluid, indicates that corrosion effects in the absence of cavitation in these investigations were negligible.

C. Lead-Bismuth Alloy at 1500°F
(References [14],[25])

The materials tested at 1500°F were identical to those tested at 500°F. The data obtained at 1500°F is displayed in Figure 6 in terms of accumulative MDP versus test duration, while Table 3 shows the rates.

BEFORE EXPOSURE	500°F.	1500°F.
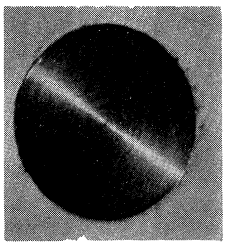	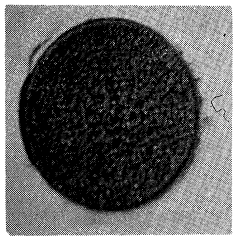	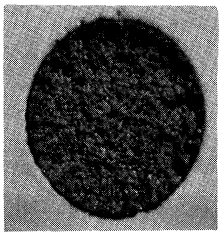
304 Stainless Steel (U-M)	304 Stainless Steel 12 Hour Exposure	304 Stainless Steel 5 Hour Exposure
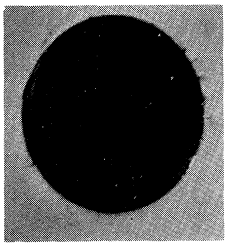	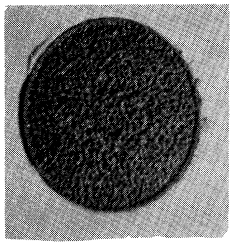	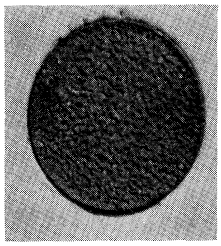
316 Stainless Steel (U-M)	316 Stainless Steel 12 Hour Exposure	316 Stainless Steel 6 Hour Exposure
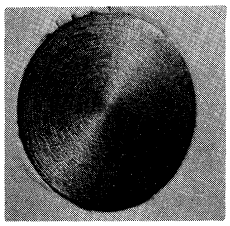	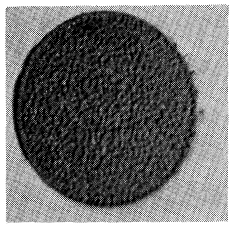	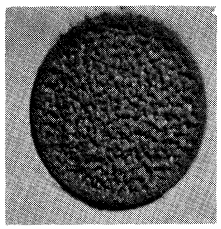
Mo-½Ti (P & W)	Mo-½Ti (P & W) 12 Hour Exposure	Mo-½Ti (P & W) 10 Hour Exposure
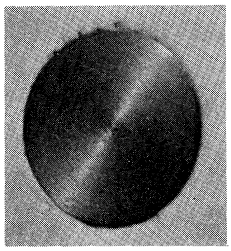	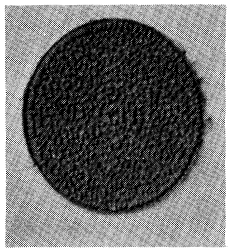	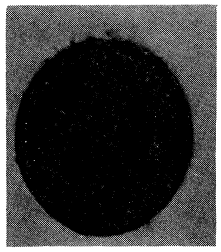
T-111 (P & W) (Ta-8W-2Hf)	T-111 (P & W) 12 Hour Exposure	T-111 (P & W) 10 Hour Exposure

Figure 5. Specimens Subjected to Cavitation Damage in Lead-Bismuth Alloy at 500°F and 1500°F

1607

BEFORE EXPOSURE	500°F.	1500°F.
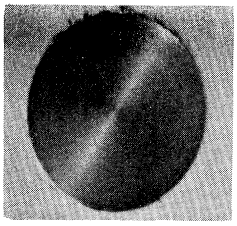	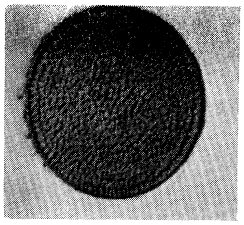	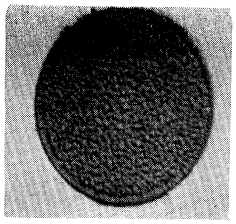
T-222(A) (P & W) (Ta-9.5W-2.5Hf-.05C)	T-222(A) (P & W) 12 Hour Exposure	T-222(A) (P & W) 10 Hour Exposure
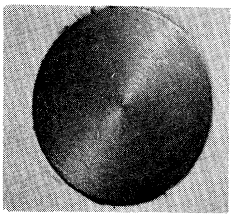	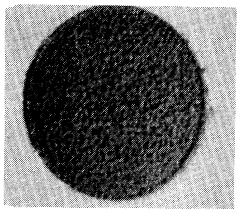	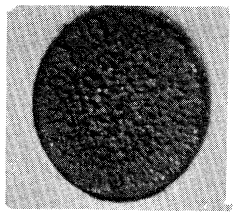
Cb-1Zr (P & W)	Cb-1Zr (P & W) 12 Hour Exposure	Cb-1Zr (P & W) 10 Hour Exposure
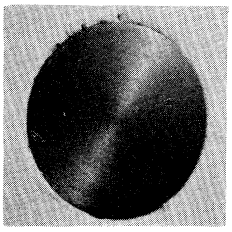	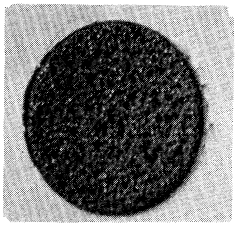	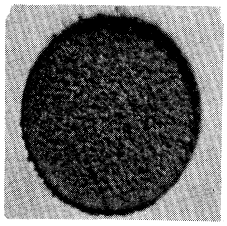
Cb-1Zr(A) (P & W)	Cb-1Zr(A) (P & W) 8 Hour Exposure	Cb-1Zr(A) (P & W) 10 Hour Exposure

Figure 5. Specimens Subjected to Cavitation Damage in Lead-Bismuth Alloy at 500°F and 1500°F

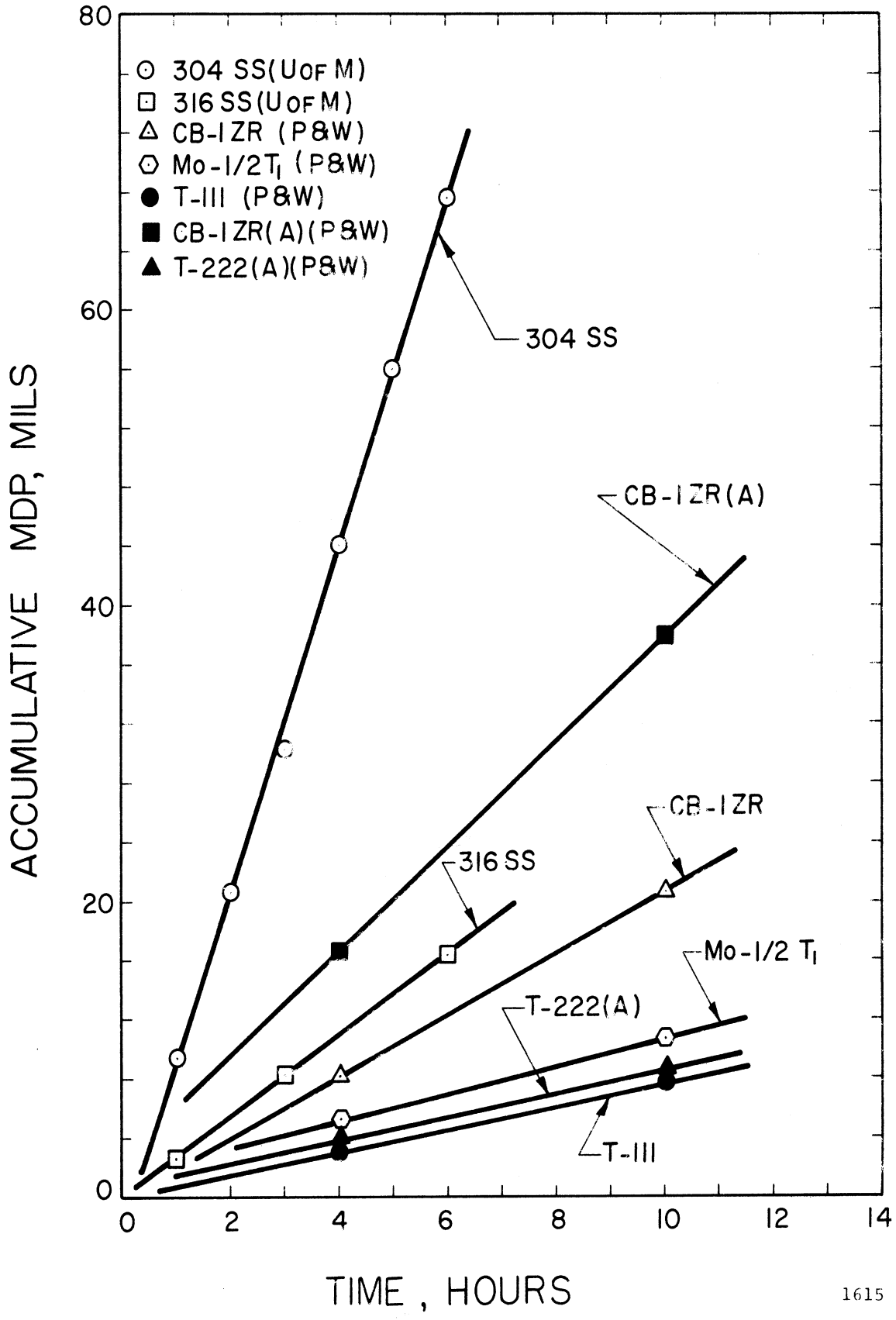

Figure 6. Effect of Cavitation Test Duration on MDP at 1500°F in Lead-Bismuth Alloy

Table 3--Summary of Cavitation Results in Lead-Bismuth at 1500°F

Material	Avg. Wt. Loss Rate	Average MDP Rate
T-111 (P & W)	57.1 mg./hr.	.84 mils/hr.
T-222(A) (P & W)	59.9	.88
Mo-1/2Ti (P & W)	42.6	1.08
Cb-1Zr (P & W)	70.0	2.07
316 SS (U-M)	83.3	2.80
Cb-1Zr(A) (P & W)	128.4	3.80
304 SS (U-M)	342.0	11.30

On the basis of MDP rates, the refractory alloy T-111 exhibited the greatest resistance to cavitation damage in this experiment, as it did at 500°F. The T-222(A) and the Mo-1/2Ti follow closely. The Cb-1Zr and the 316 stainless steel rated well behind the tantalum and molybdenum alloys, while both the Cb-1Zr(A) and the 304 stainless steel were considerably less resistant than the others. Both were grossly damaged, especially the 304 stainless steel, where the test was concluded after only five hours, whereas ten hours were used for the others. Again the rate of erosion for each individual material was approximately constant during most of the test.

As expected, the refractory alloys T-111, T-222(A), Mo-1/2Ti, and Cb-1Zr are far superior to the stainless steels with respect to resistance to cavitation erosion at 1500°F.

Photographs of the test specimens before and after exposure at both 500°F and 1500°F are presented in Figure 5 (previously cited) for comparison.

Detailed examination of the exponential horn, container vessel, and the sides of the various specimens again did not indicate any evidence of corrosion.

D. Comparison of Lead-Bismuth Results at 500°F and 1500°F

The tantalum alloys, T-111 and T-222(A), were the most resistant to cavitation at both 500°F and at 1500°F. The Mo-1/2Ti ranks third at both temperatures. Note the poor relative performance of the stainless steels at 1500°F as compared with 500°F. This is, of course, to be

expected from a consideration of the effect of temperature upon their respective mechanical properties. The differences in the amount of attack on the various specimens and the effect of temperature can readily be seen in the photographs of Figure 5.

For each material tested the amount of damage sustained by the specimen at 1500°F was greater than that sustained at 500°F for constant testing time, as expected. The difference was, of course, much greater for the stainless steels than for the refractories since their mechanical properties are much more temperature dependent.

The effect of temperature on the damage rates is shown specifically in Figure 7. It is almost negligible on the T-111, T-222(A), and Mo-1/2Ti, while its effect on the stainless steels is quite dramatic, as evidenced by the slopes of the appropriate curves.

E. Mercury at 500°F

Table 4 summarizes the cavitation results obtained on the eight materials tested in mercury at 500°F. Figure 8 shows accumulative MDP versus test duration.

On the basis of either weight loss rate or MDP rate T-111 is again the most cavitation resistant of the materials tested, while the T-222(A) is again next (~seven per cent less resistant). The hot-rolled carbon steel, 316 stainless steel, and 304 stainless steel rank third, fourth, and fifth, respectively. Three refractory materials: Mo-1/2Ti, Cb-1Zr, and Cb-1Zr(A), were the least resistant, with the Cb-1Zr(A) considerably the worst. These three materials suffered damage

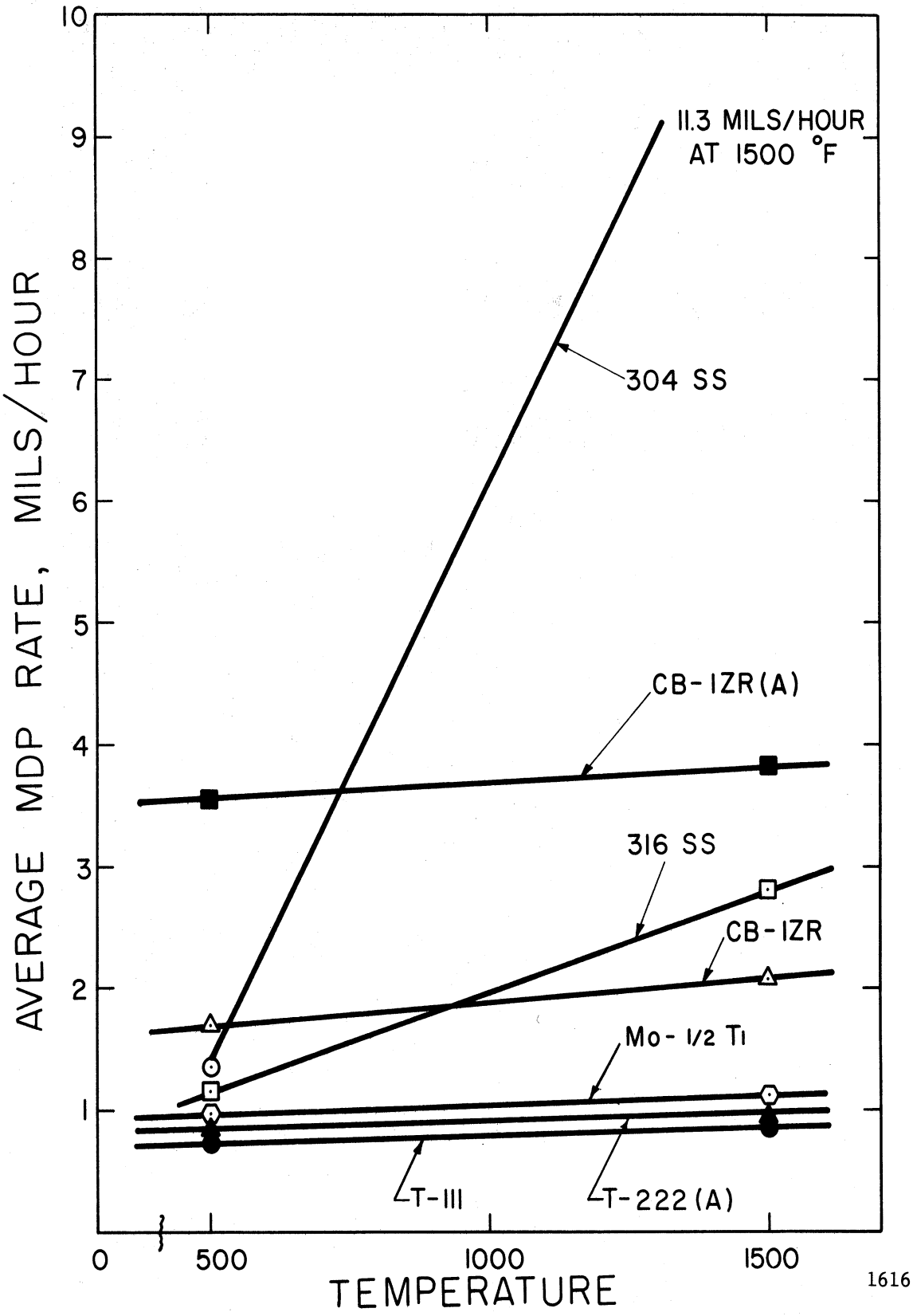

Figure 7. Effect of Temperature on Cavitation Resistance in Lead-Bismuth Alloy

Table 4--Summary of Cavitation Results in Mercury at 500°F

Material	Avg. Wt. Loss Rate	Average MDP Rate
T-111 (P & W)	29.48 mg./hr.	.43 mils/hr.
T-222(A) (P & W)	31.52	.46
Carbon Steel (U-M)	18.60	.61
316 SS (U-M)	19.01	.63
304 SS (U-M)	20.83	.69
Mo-1/2Ti (P & W)	43.16	1.09
Cb-1Zr (P & W)	81.85	2.43
Cb-1Zr(A) (P & W)	125.78	3.73

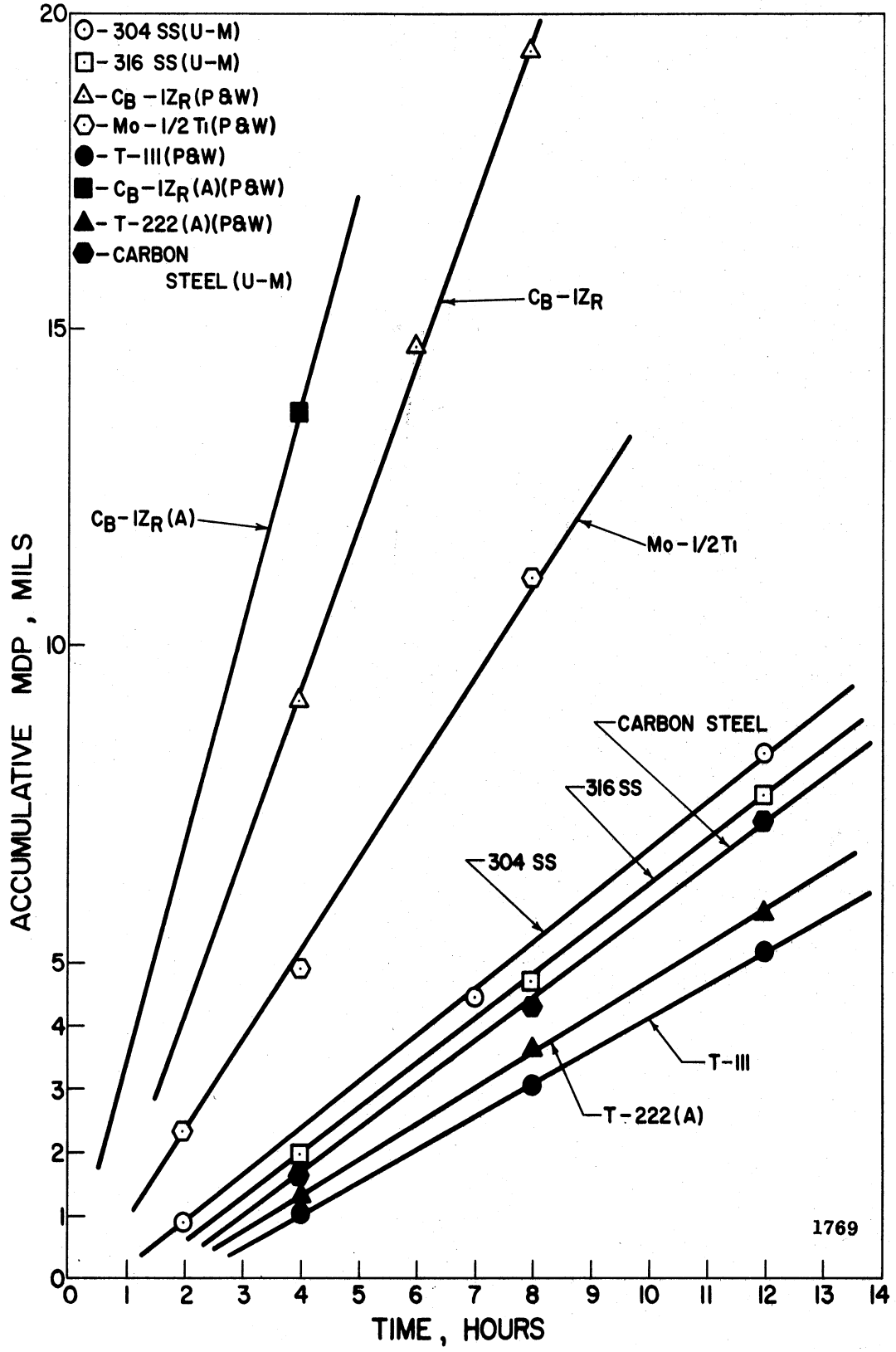

Figure 8. Effect of Cavitation Test Duration on MDP at 500°F in Mercury

ranging from three to eight times that of the tantalum-base alloys. Again the rate of erosion for each individual material is approximately constant during the test.

Photographs of the specimens at the conclusion of the test are shown in Figure 9. The materials are arranged in order of decreasing resistance to cavitation damage. Note the severe pitting of the Mo-1/2Ti, Cb-1Zr, and Cb-1Zr(A) surfaces. In all cases the damage is relatively uniform over the specimen face rather than in the form of individual, isolated, deep pitting. It is felt that the approximately constant rate of erosion noted for all the materials tested in mercury at 500°F is due to this uniform damage pattern, and the fact that the area presented to the collapsing bubble cloud is approximately constant for the duration of the test. A similar comment applies to the lead-bismuth results. A photograph of a 304 stainless steel specimen before exposure is included in Figure 9 and serves to indicate a representative initial surface condition for all specimens.

Detailed examination of the exponential horn, container vessel, and the sides of the various specimens again did not indicate any evidence of corrosion.

F. Mercury at 70°F

Table 5 summarizes the cavitation results obtained in mercury at 70°F, while Figure 10 is a plot of accumulative MDP versus test duration for the nine materials tested.

The 304 stainless steel and 316 stainless steel were the most resistant to cavitation at 70°F based on average MDP rate, differing by

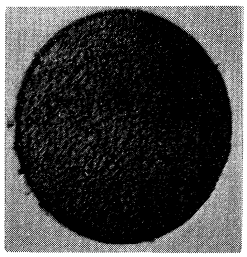

(1) T-111(P & W)
12 Hour Exposure

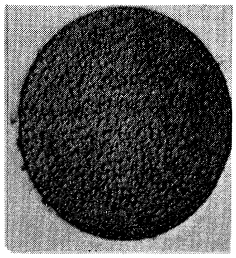

(2) T-222(A)(P & W)
12 Hour Exposure

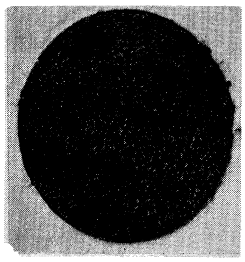

(3) Carbon Steel(U-M)
12 Hour Exposure

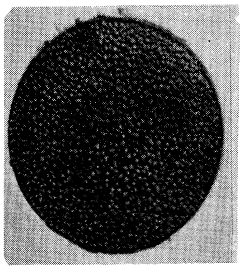

(4) 316 SS(U-M)
12 Hour Exposure

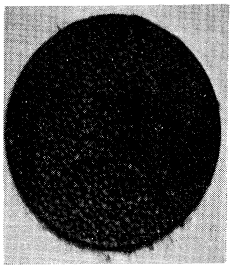

(5) 304 SS(U-M)
12 Hour Exposure

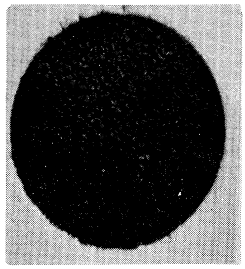

(6) Mo-1/2Ti(P & W)
12 Hour Exposure

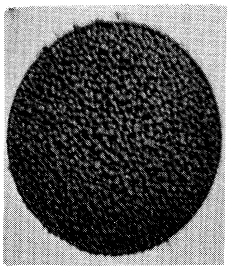

(7) Cb-1Zr(P & W)
8 Hour Exposure

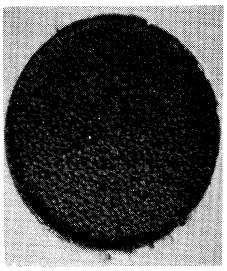

(8) Cb-1Zr(A)(P & W)
8 Hour Exposure

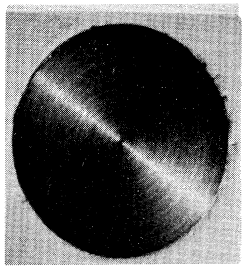

304 SS(U-M)
Before Exposure

Figure 9. Specimens Subjected to Cavitation Damage in Mercury at 500°F

1770

Table 5--Summary of Cavitation Results in Mercury at 70°F

Material	Avg. Wt. Loss Rate	Average MDP Rate
304 SS (U-M)	9.82 mg./hr.	.32 mils/hr.
316 SS (U-M)	9.88	.33
T-111 (P & W)	23.71	.35
T-222 (P & W)	28.92	.43
Mo-1/2Ti (P & W)	22.58	.57
Cb-1Zr (P & W)	31.04	.92
Carbon Steel (U-M)	31.17	1.03
Cb-1Zr(A) (P & W)	54.22	1.61
Plexiglas (U-M)	19.00	3.99

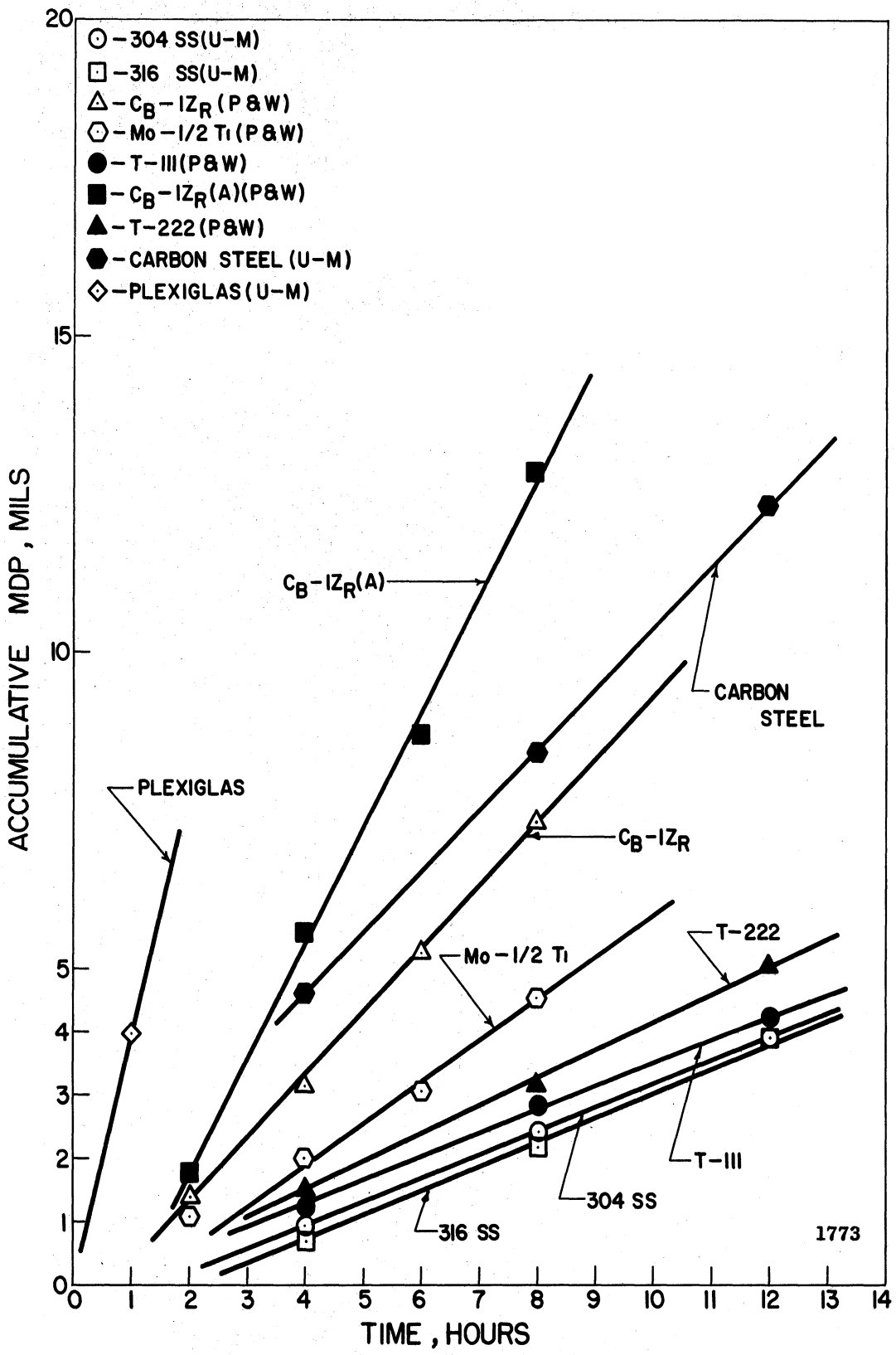

Figure 10. Effect of Cavitation Test Duration on MDP at 70°F in Mercury

only three per cent. The alloys T-111 and T-222 were six per cent and 30 per cent less resistant than the stainless steels, respectively, while the Mo-1/2Ti was 80 per cent less resistant. The Cb-1Zr, hot-rolled carbon steel, and Cb-1Zr(A) all were considerably less resistant, with MDP rates approximately three to five times greater than for the stainless steels. The Plexiglas suffered the greatest average MDP rate (about ten times that of the stainless steels). Once again the rate of erosion for each individual material is approximately constant.

Figure 11 shows photographs of the test specimens at the conclusion of the test. The materials are arranged in order of decreasing resistance to cavitation damage. Again the damage is relatively uniform over the specimen face. A photograph of a 304 stainless steel specimen before exposure is included to indicate initial surface condition.

No evidence of corrosion was noted on the test specimens.

G. Comparison of Mercury Results at 70°F and 500°F

The most cavitation-resistant materials at 70°F were the stainless steels with the tantalum-base alloys ranking third and fourth. At 500°F the superior mechanical properties of the tantalum-base alloys at this moderately elevated temperature are already evident as the T-111 and T-222(A) rank first and second, respectively. The hot-rolled carbon steel, 316 stainless steel, and 304 stainless steel rank third, fourth, and fifth, respectively, at 500°F. The Mo-1/2Ti, Cb-1Zr, and Cb-1Zr(A) all maintained the same relative position at both test temperatures. The hot-rolled carbon steel which had fared well at 500°F with a third

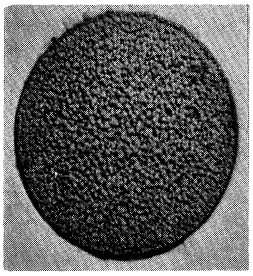

(1) 304 SS(U-M)
12 Hour Exposure

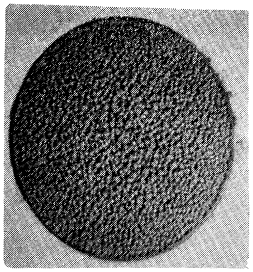

(2) 316 SS(U-M)
12 Hour Exposure

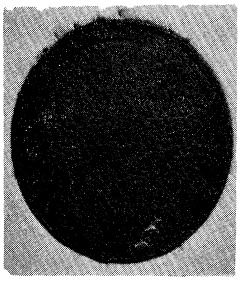

(3) T-111(P & W)
12 Hour Exposure

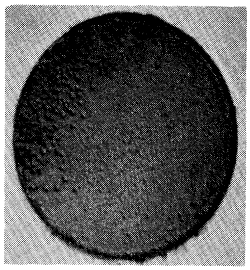

(4) T-222(P & W)
12 Hour Exposure

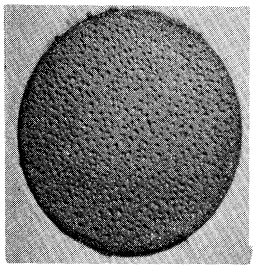

(5) Mo-1/2Ti(P & W)
8 Hour Exposure

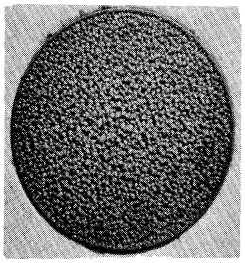

(6) Cb-1Zr(P & W)
8 Hour Exposure

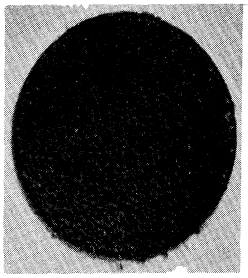

(7) Carbon Steel(U-M)
12 Hour Exposure

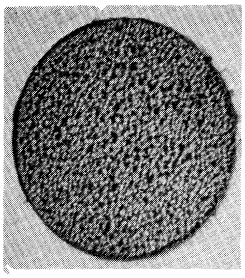

(8) Cb-1Zr(A)(P & W)
8 Hour Exposure

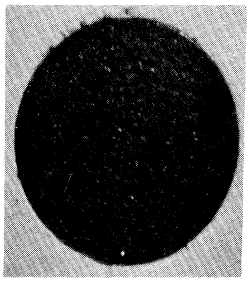

(9) Plexiglas(U-M)
1 Hour Exposure

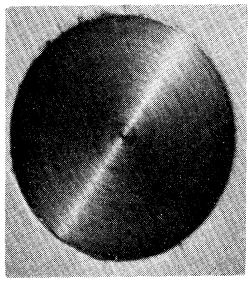

304 SS(U-M)
Before Exposure

1774

Figure 11. Specimens Subjected to Cavitation Damage in Mercury at 70°F

ranking was damaged almost 70 per cent more at 70°F. This apparently anomalous behavior is due to the fact that several of the mechanical properties of the hot-rolled carbon steel such as tensile strength and yield strength are actually significantly greater at 500°F than at 70°F. The reverse is true of the stainless steels.

With the exception of the hot-rolled carbon steel, all of the materials tested sustained greater damage at 500°F than at 70°F, as would be expected. The stainless steel damage rate was about doubled over this moderate temperature range, and the T-111 increased about 23 per cent. The damage rates for the Mo-1/2Ti, Cb-1Zr, and Cb-1Zr(A) were increased by a factor of two to three. The effect on the T-111 and T-222 is almost negligible. Figure 12 shows these effects for the mercury tests.

H. Water at 70°F

1. General--The 24 materials tested in water at 70°F have been divided into three subsets. The first consists of those materials that have also been tested in mercury and lead-bismuth, namely 304 stainless steel, 316 stainless steel, T-111, T-222, Mo-1/2Ti, hot-rolled carbon steel, Cb-1Zr, and Cb-1Zr(A). The second subset consists of the three aluminum alloys and Plexiglas, while the third includes twelve alloys and heat-treat combinations of Cu, Cu-Zn, Cu-Ni, and Ni. The second and third subsets contain materials that have been tested only in water (with the exception of Plexiglas which was also tested in mercury at 70°F).

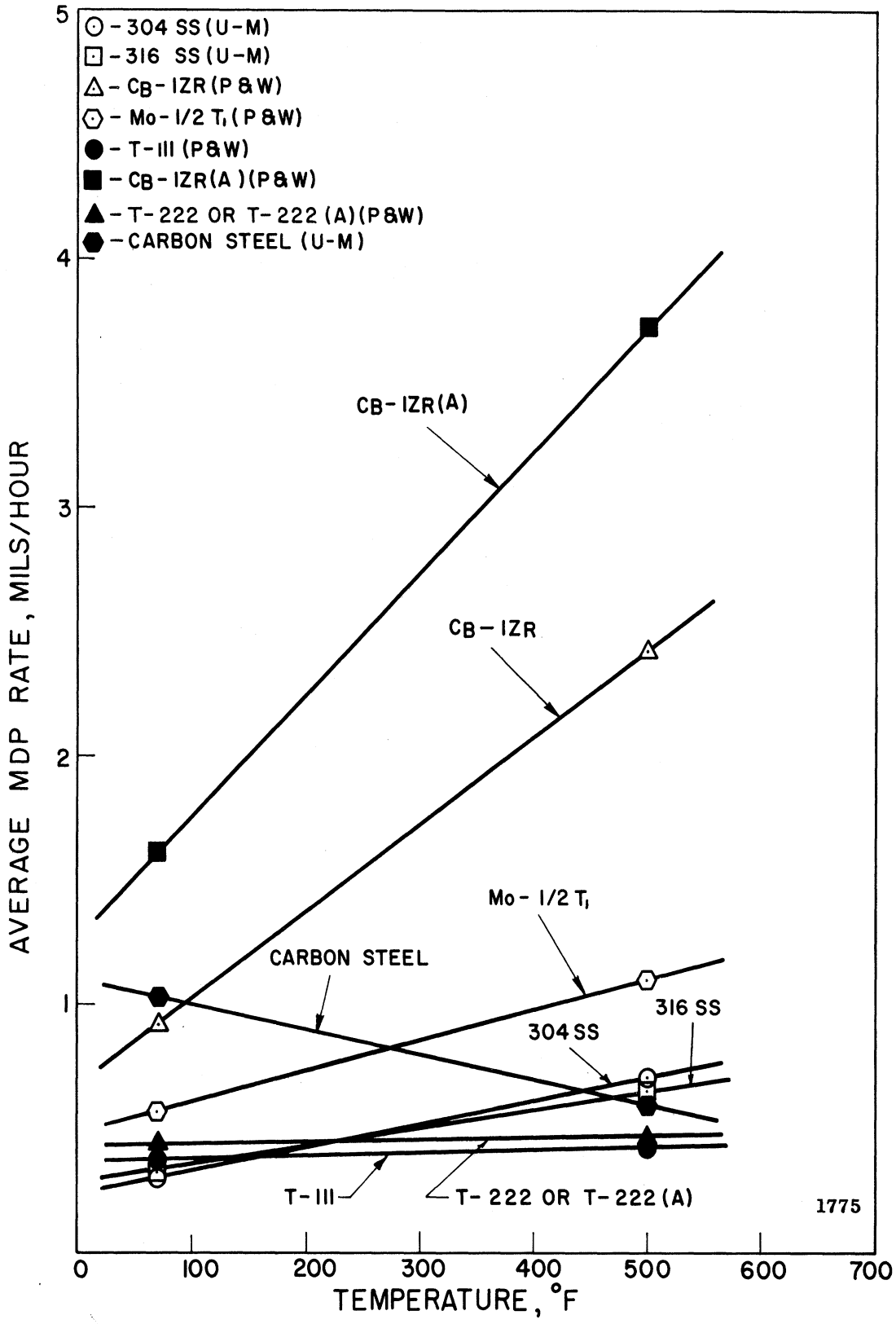

Figure 12. Effect of Temperature on Cavitation Resistance in Mercury

2. Subsets One and Two--Table 6 summarizes the damage data in water at 70°F for these materials. Figure 13 is a plot of accumulative MDP versus test duration for the eight materials contained in subset one. Figure 14 is the corresponding plot for subset two.

On the basis of average MDP rate T-222 is the most cavitation resistant of the materials contained in subsets one and two. T-111, ranking second, suffered about three times more damage than T-222. Mo-1/2Ti, 316 stainless steel, 304 stainless steel, Cb-1Zr, Cb-1Zr(A), and hot-rolled carbon steel follow in that order. The aluminum alloys and Plexiglas were the least resistant among these materials. Considering only the three aluminum alloys, the 2024-T351 alloy was the most resistant while the very soft 1100-0 alloy sustained the greatest damage.

Figure 13 indicates that the rate of erosion for the T-222, T-111, Mo-1/2Ti, 316 stainless steel, and 304 stainless steel is approximately constant over the test duration, while the rate of erosion for the Cb-1Zr, Cb-1Zr(A), and the hot-rolled carbon steel is approximately constant during the early stages of the test and then begins to decrease as the accumulative weight loss and the accumulative MDP increase to larger values. Examination of the specimens indicated that those materials with a constant damage rate exhibit a fairly uniform and fine-structure damage pattern, whereas those showing a non-linear response are characterized by surface damage consisting primarily of heavy, isolated, deep pitting. This latter pattern would result in a greatly reduced bubble population, thus producing greatly reduced damage rates.[15]

Table 6--Summary of Cavitation Results in Water at 70°F - Subsets One and Two

Material	Avg. Wt. Loss Rate	Average MDP Rate
T-222 (P & W)	1.05 mg./hr.	.02 mils/hr.
T-111 (P & W)	4.33	.06
Mo-1/2Ti (P & W)	3.49	.09
316 SS (U-M)	2.81	.09
304 SS (U-M)	3.04	.10
Cb-1Zr (P & W)	5.10	.15
Cb-1Zr(A) (P & W)	6.10	.18
Carbon Steel (U-M)	7.08	.23
2024-T351 Al (U-M)	6.13	.57
6061-T651 Al (U-M)	7.73	.72
Plexiglas (U-M)	6.60	1.39
1100-0 Al (U-M)	28.90	2.70

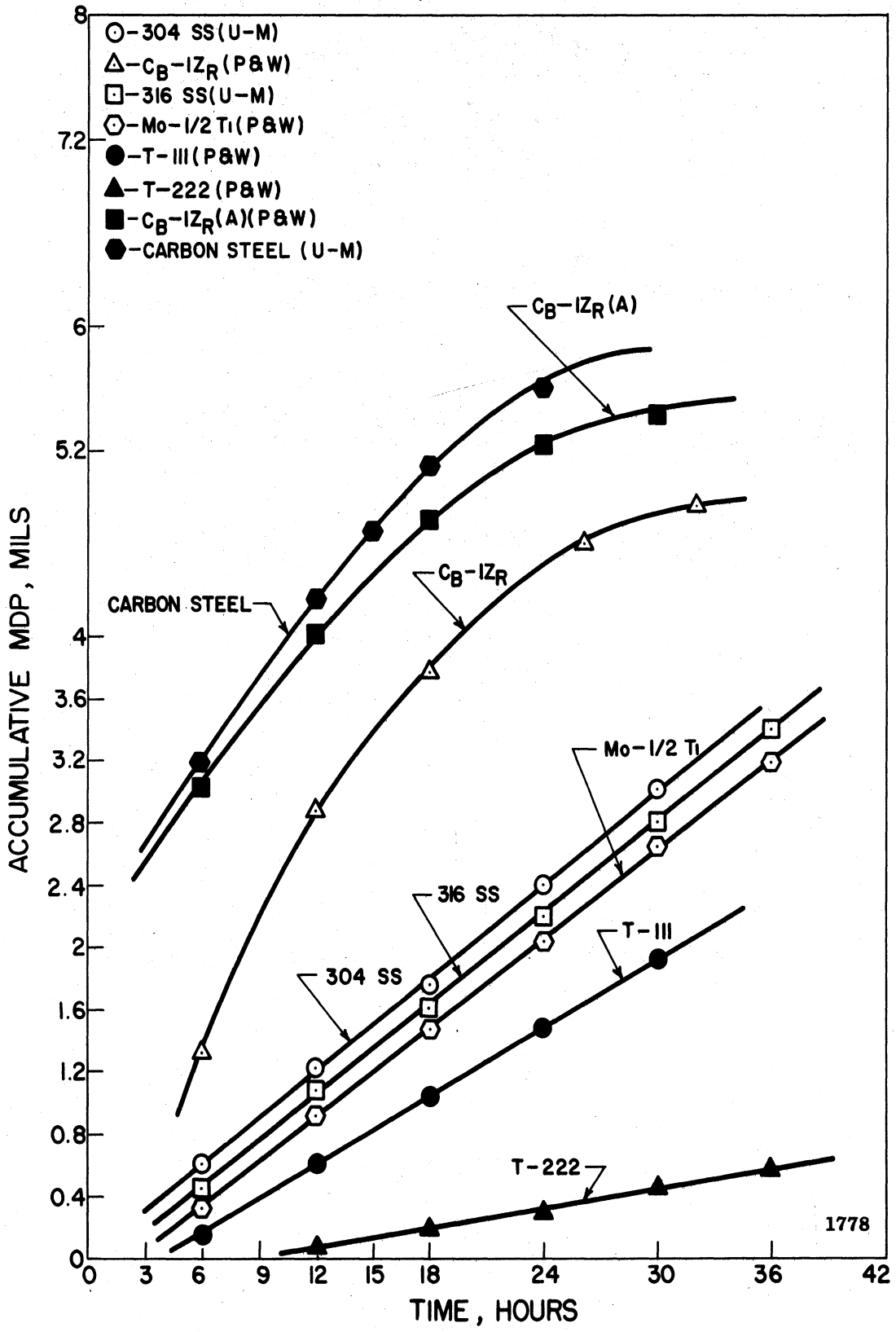

Figure 13. Effect of Cavitation Test Duration on MDP at 70°F in Water - Subset One

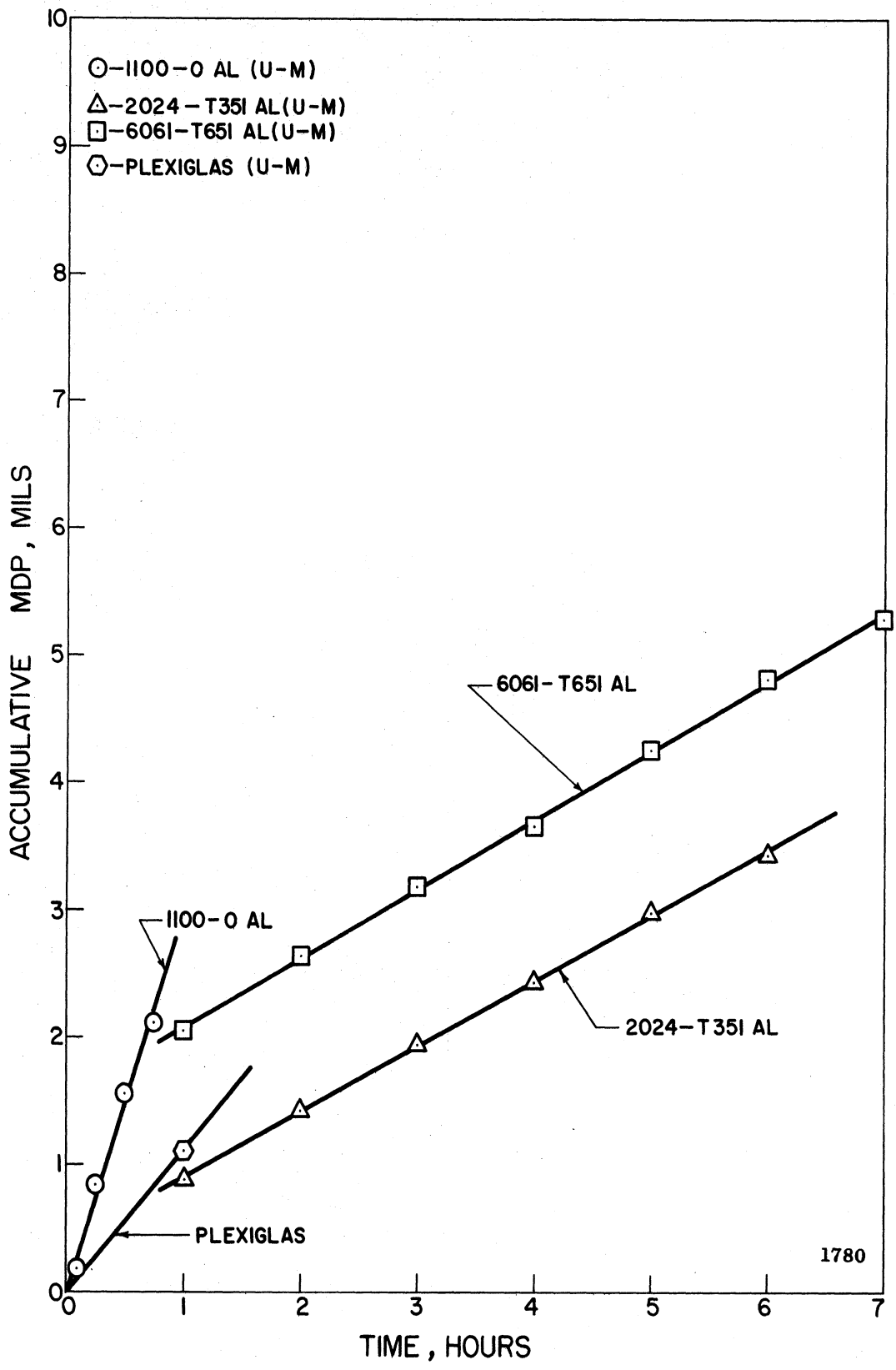

Figure 14. Effect of Cavitation Test Duration on MDP at 70°F in Water - Subset Two

Hence, for this type of pitting, one would expect the erosion rate to decrease as the total weight loss or MDP increased, as clearly pointed out in a recent paper by Plesset and Devine.[15]

Figure 15 shows photographs of the test specimens in subset one after the test, arranged in order of decreasing resistance. Note the deep, isolated pitting of the Cb-1Zr, Cb-1Zr(A), and hot-rolled carbon steel surfaces. A photograph of a 304 stainless steel specimen before exposure is included in Figure 15 and serves to indicate a representative initial surface condition for all the specimens tested.

Figure 14 shows that the rate of erosion for the three aluminum alloys is approximately constant during the test, in spite of the deep, isolated pitting of the type which in the previous materials corresponded to a non-linear damage rate. The explanation for this anomaly is not at present known.

Photographs of the test specimens in subset two at the conclusion of the cavitation experiment are presented in Figure 16. A photograph of a 2024-T351 aluminum specimen before exposure is included for comparison.

3. Subset Three--Table 7 summarizes the cavitation results obtained in water at 70°F for the materials in subset three, namely the twelve Cu, Cu-Zn, Cu-Ni, and Ni heat-treat and alloy combinations. The various heat-treats of a given material are grouped together. Figure 17 shows accumulative MDP versus test duration for the six Cu and Ni materials, while Figure 18 is the corresponding plot for the six Cu-Zn and Cu-Ni materials.

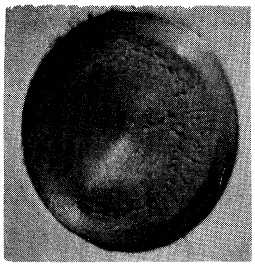

(1) T-222(P & W)
36 Hour Exposure

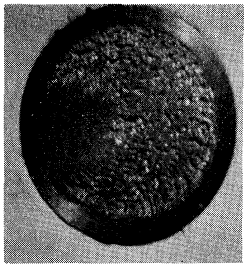

(2) T-111(P & W)
30 Hour Exposure

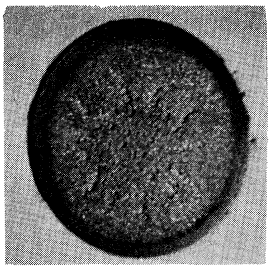

(3) Mo-1/2Ti(P & W)
36 Hour Exposure

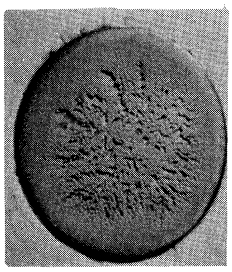

(4) 316 SS(U-M)
36 Hour Exposure

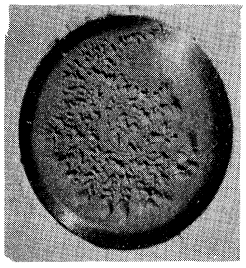

(5) 304 SS(U-M)
30 Hour Exposure

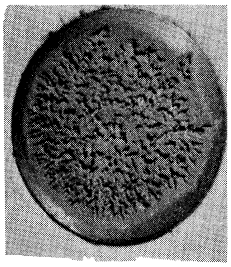

(6) Cb-1Zr(P & W)
32 Hour Exposure

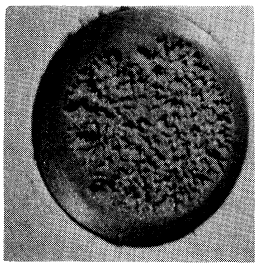

(7) Cb-1Zr(A)(P & W)
30 Hour Exposure

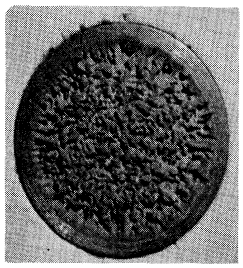

(8) Carbon Steel(U-M)
21 Hour Exposure

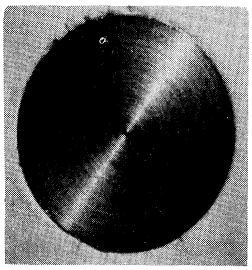

304 SS(U-M)
Before Exposure

Figure 15. Specimens Subjected to Cavitation Damage in Water at 70°F - Subset 1

1781

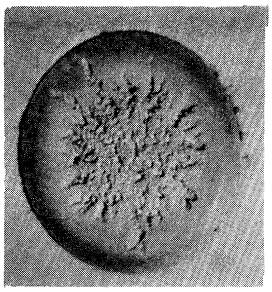

(1) 2024-T351 Al(U-M)
6 Hour Exposure

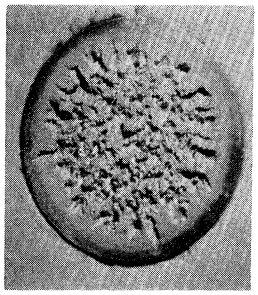

(2) 6061-T651 Al(U-M)
8 Hour Exposure

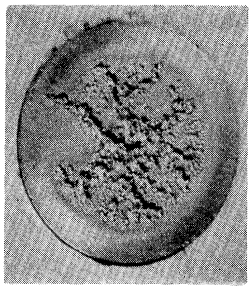

(3) 1100-0 Al(U-M)
45 Minute Exposure

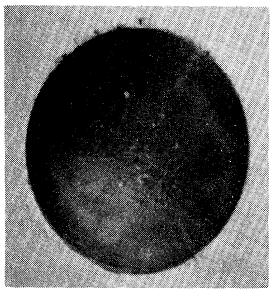

Plexiglas(U-M)
30 Minute Exposure

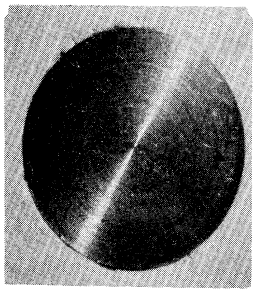

2024-T351 Al(U-M)
Before Exposure

1782

Figure 16. Specimens Subjected to Cavitation Damage in Water at 70°F - Subset 2

Table 7--Summary of Cavitation Results in Water at 70°F - Subset Three

Material	Avg. Wt. Loss Rate	Average MDP Rate
Cu, cold-worked	32.83 mg./hr.	.95 mils/hr.
Cu, 900°F anneal	35.37	1.02
Cu, 1500°F anneal	33.32	.95
Cu-Ni, cold-worked	24.18	.70
Cu-Ni, 1300°F anneal	21.97	.63
Cu-Ni, 1800°F anneal	16.25	.47
Cu-Zn, cold-worked	12.74	.38
Cu-Zn, 850°F anneal	23.88	.72
Cu-Zn, 1400°F anneal	22.78	.68
Ni, cold-worked	15.27	.44
Ni, 1100°F anneal	20.25	.58
Ni, 1600°F anneal	16.69	.48

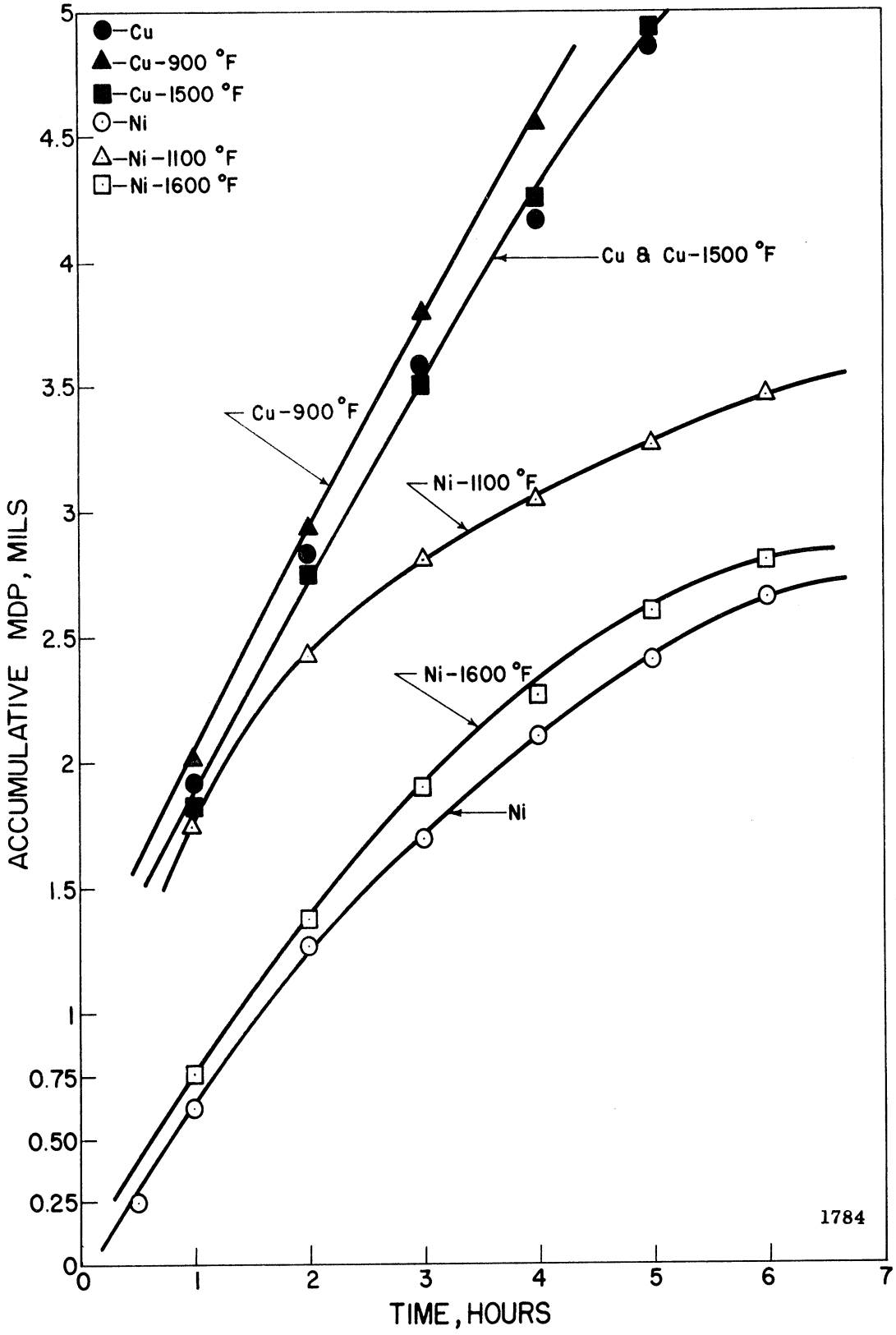

Figure 17. Effect of Cavitation Test Duration on MDP at 70°F in Water - Subset Three (Cu and Ni)

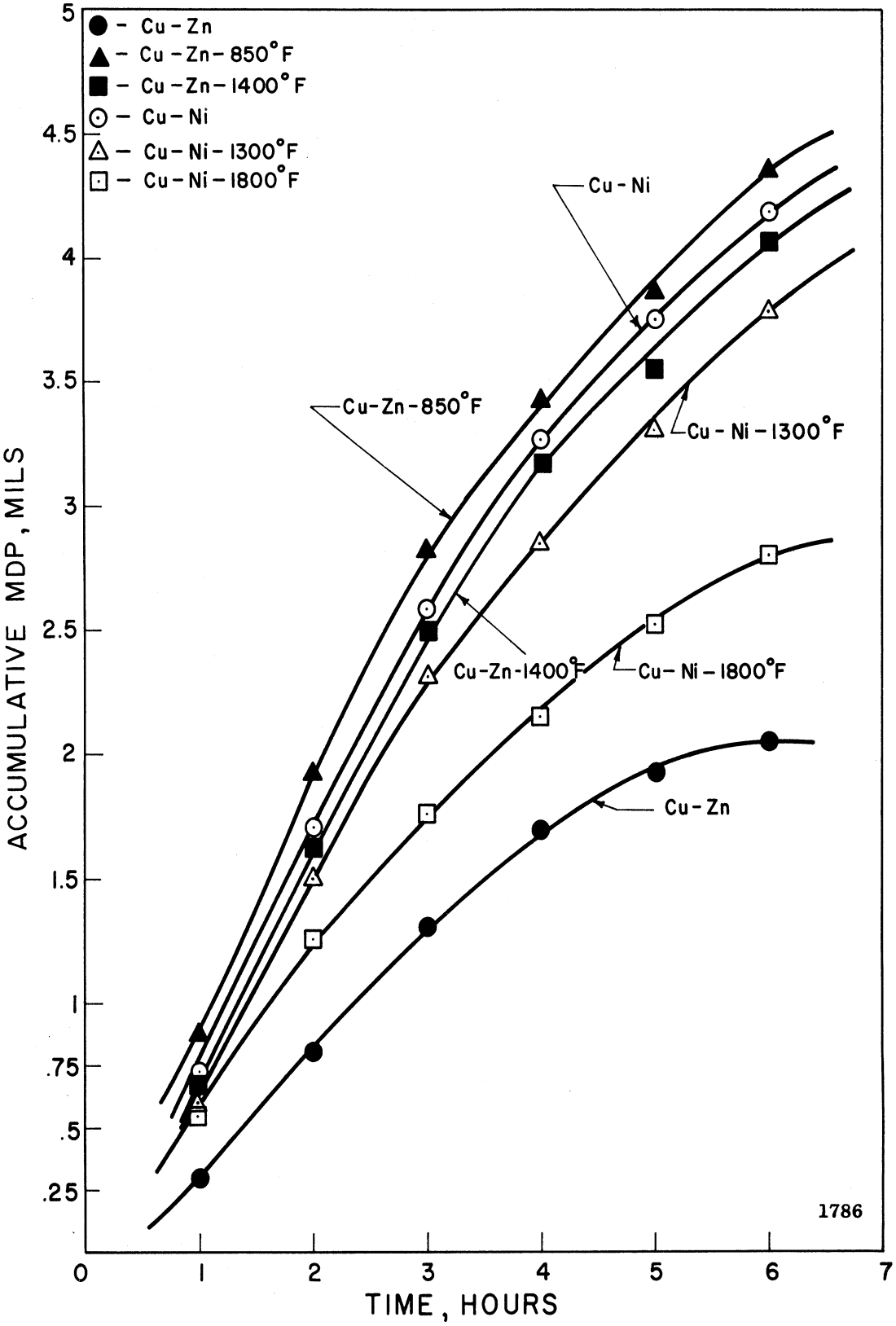

Figure 18. Effect of Cavitation Test Duration on MDP at 70°F in Water - Subset Three (Cu-Zn and Cu-Ni)

Among these, on the basis of average MDP rate the Cu-Zn (60 per cent cold-worked) was the most resistant. Ni (75 per cent cold-worked) ranked second, while the Cu-Ni (1800°F anneal, one hour) and Ni (1600°F anneal, one hour) were third and fourth. The three copper heat-treats were the least resistant to cavitation damage in subset three with the Cu (900°F anneal, one hour) ranking last.

Considering only the three copper specimens, the cold-worked material was most cavitation resistant while the high-temperature heat-treat ranked second and the low-temperature heat-treat was third. Identical rankings apply to the three Cu-Zn specimens and the three Ni specimens. For Cu-Ni the high-temperature heat-treated specimen was the most cavitation resistant followed by the low-temperature heat-treated material and the cold-worked specimen in that order.

Figures 17 and 18 indicate that the erosion rate for the subset three materials is generally <u>not</u> constant. This is believed due to the pattern of the surface damage which for these materials is characterized by heavy, isolated, deep pitting (Figure 19). As previously discussed,[15] such a condition would result in changes in flow geometry giving a greatly reduced bubble population. This preferential damage of the surface may be caused by non-uniformity of applicable mechanical properties, resulting in a substantial interaction between mechanical and chemical effects through the setting up of galvanic cells. This may be consistent with the fact that for stainless steel a uniform pitting distribution is obtained in lead-bismuth and mercury, while in water deep, isolated pitting results.

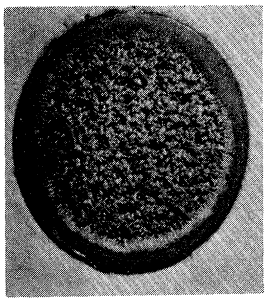

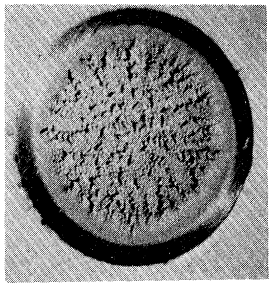

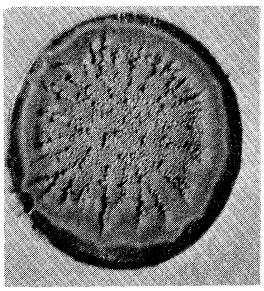

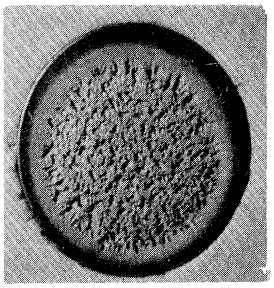

Cu-Ni(1300°F anneal)(U-M)
6 Hour Exposure

Cu-Zn(1400°F anneal)(U-M)
6 Hour Exposure

1787

Figure 19. Specimens Subjected to Cavitation Damage in Water at 70°F - Subset Three

The lack of similarity in damage pattern may also be partially due to the fact that NPSH has not been modeled between tests so that similarity of flow regime would not be expected.

In all of the tests conducted in water, only the hot-rolled carbon steel specimen showed definite visual indications of corrosion. Hence the results for this material are significantly influenced by both corrosion and mechanical attack.

Comparison of Mercury and Water Results at 70°F

A comparison of the results obtained in mercury and water at the same temperature (70°F) is useful to observe effects of fluid properties on cavitation damage. This particular case affords an observation of the effect of density variation in a vibratory test conducted under fixed static suppression pressure. The comparison is made on the basis of average MDP rate (see Tables 5 and 6).

1) Several differences exist in the comparative ratings of materials between the two fluids. In mercury, the stainless steels and tantalum-base alloys were the most resistant to cavitation damage and only differed in this respect by about 25 per cent. In water, the tantalum-base alloys were the most resistant, while the stainless steels suffered damage two times to five times greater than the T-111 and T-222. The Mo-1/2Ti ranked third in water and fifth in mercury. However, the first five rankings are occupied by the same materials in both fluids. The Cb-1Zr, carbon steel, Cb-1Zr(A), and Plexiglas suffered the most

damage and had comparable rankings in both fluids except for the carbon steel which ranked seventh in mercury and eighth in water. This could have been due to the additional corrosion suffered by the carbon steel in water.

2) Damage in mercury was 3 to 20 times greater than in water. The stainless steels, in particular, suffered about three times as much damage in mercury as in water. Note that the comparison is on the basis of equal static suppression pressures rather than equal NPSH. For a comparison with equal NPSH, it is likely that the mercury damage would be proportionately increased, since the static suppression pressure for mercury would then be 13.6 times as great.

3) The stainless steels were the most cavitation resistant materials in mercury, while the tantalum-base alloys, T-111 and T-222, were far superior in water. This may be due to the change in character of damage incurred by the stainless steel between the two fluids, as previously discussed. The Plexiglas was the least resistant in both fluids, as opposed to the venturi tests where it was quite resistant in water but poor in mercury. This may indicate that materials which rely to some extent on a superior yield deflection range for their protection (as rubberized coatings and also Plexiglas in the present tests) are suitable in relatively low intensity cavitation fields, but fail under more intense attack. This observation is at least consistent with much field experience.

Presumably the primary cause of the greater damage suffered by all the materials in mercury than in water is the much greater density of mercury. The pressures generated by bubble collapse are theoretically roughly proportional to fluid density, if the suppression heads seen by the bubbles and the kinetic behavior of the horn were the same in both fluids. This may be approximately the case in the present tests since the major contribution to the suppression head at the start of bubble collapse is the dynamic portion of the head caused by the horn motion. This portion would be the same for all tests, although the static suppression heads differ by the density ratio, since constant static suppression pressure was maintained.

K. Comparison of Mercury and Lead-Bismuth Results at 500°F

A further comparison of fluid effects can be obtained between the mercury and lead-bismuth 500°F tests (see Tables 2 and 4). For this case the applicable properties of the fluids do not differ widely (Table 8). Again the comparison is made on the basis of average MDP rate.

1) For both the lead-bismuth and the mercury tests the materials investigated had almost identical comparative ratings (as opposed to the water-mercury comparison). The only exception was Mo-1/2Ti (P & W) which ranked third in lead-bismuth and fifth in mercury.

2) Any given material tested in both fluids suffered damage which was of the same order of magnitude. This is not surprising considering the similarity of the fluids.

Table 8--Fluid Properties Data at Various Temperatures

(Taken from References [23] and [24])

Fluid Property	Fluid				
	Water 70°F	Mercury 70°F	Mercury 500°F	Pb-Bi 500°F	Pb-Bi 1500°F
Acoustic Impedance (AI) (lbm./ft.^{2}sec.)	$.299 \times 10^6$	4.03×10^6	3.85×10^6	3.08×10^6	2.86×10^6
Density (ρ) (g./cc.)	1.0	13.55	12.98	10.38	9.64
Surface Tension (σ) (dynes/cm.)	72.8	465.0	419.0	397.0	367.0
Net Positive Suction Head (NPSH) (feet)	36.5	2.7	2.8	3.5	3.8
Bulk Modulus (B) (psi)	$.31 \times 10^6$	4.11×10^6	3.94×10^6	3.16×10^6	2.92×10^6
Kinematic Viscosity (γ) (ft.^{2}/hour)	.039	.0044	.0030	.0064	.0047
Specific Heat (C_p) (cal./g./°C)	1.00	.033	.032	.035	.035
Thermal Conductivity (k) (cal./sec.cm.°C)	1.41×10^{-3}	.021	.030	.025	...
Heat of Vaporization (HV) (cal./g.)	585	69.7	69.7	...	...
Vapor Pressure (p_v) (psi)	0.36	0	1.93	0	0

3) The T-111, T-222(A), 316 stainless steel, and 304 stainless steel all suffered less damage in the mercury than in the lead-bismuth alloy, while the Mo-1/2Ti, Cb-1Zr, and Cb-1Zr(A) suffered more in mercury. However, the differences were not great in any case.

CHAPTER IV

MECHANICAL PROPERTIES DATA

In order to obtain a meaningful correlation between the cavitation resistance of the various materials tested, their mechanical properties, and suitable fluid coupling parameters, it is absolutely essential that the applicable mechanical properties such as tensile strength, yield strength, engineering strain energy, true strain energy, hardness, elongation, reduction in area, and elastic modulus be measured at the test temperatures using tensile bars machined from the same stock as were the cavitation specimens. Otherwise the variations between material lots due to differences in heat-treat, cold work, etc., are too large to allow useful results. Accordingly, for a given material all cavitation test specimens, tensile bars, and special hot hardness specimens were machined from the same piece of bar stock. In the case of the Cu, Cu-Zn, Cu-Ni, and Ni materials that were available only in sheet stock, flat tensile specimens were fabricated and tested.

The mechanical properties data for the stainless steels and refractory materials were determined at 70°F and 500°F at Pratt & Whitney Aircraft (CANEL). All the refractory materials tested in this program were supplied by Pratt & Whitney Aircraft (CANEL), whereas the stainless steels were supplied by this laboratory. The results of the

portion of the mechanical properties determination program conducted at Pratt & Whitney were supplied to this laboratory by private communication[16] and are tabulated in Tables 9 and 10.

The mechanical properties data for the aluminum alloys, carbon steel, Plexiglas, and the Cu, Cu-Zn, Cu-Ni, and Ni materials were determined at room temperature in the Department of Chemical and Metallurgical Engineering laboratories at the University of Michigan and were reported earlier.[17,18] The mechanical properties for carbon steel were also determined at 500°F. The data obtained from these tests are listed in Table 11.

The mechanical properties data determined by Pratt & Whitney Aircraft and the University of Michigan consist of values of tensile strength (TS), yield strength (YS), engineering strain energy (ESE), true strain energy (TSE), hardness (H), per cent elongation (ELON), per cent reduction in area (RA), and elastic modulus (E). Most of these have been suggested at one time or another as possible correlating parameters for cavitation damage. Most recently, both abroad[19] and in the United States,[20] strain energy concepts have been advanced.

The "engineering strain energy" is based on the "approximate" or engineering stress-strain curve and is equal to the area under this curve as it is produced by a standard tensile machine.[18] Two values of "true strain energy" were used in our correlations (and listed in Tables 9, 10, and 11) and are based on approximations to the true stress-strain curve.[18] The first value of true strain energy, denoted by TSEE, takes into account elongation of the test specimen as a whole in computing the

Table 9--Mechanical Properties Data at 70°F From Pratt & Whitney Aircraft (CANEL)

Material	Tensile Strength psi	Yield Strength psi	Eng. Strain Energy psi	True Strain Energy psi		DPH Hardness 1.1 Kg.	Elongation %	Area Reduction %	Elastic Modulus psi
304 SS	94,500	64,700	57,300	41,300	47,500	237	63.8	77.9	29.0×10^6
316 SS	87,200	63,600	48,850	38,200	49,500	227	57.8	80.3	29.0×10^6
T-111	131,600	124,900	16,750	16,000	68,600	308	14.8	80.4	28.0×10^6
T-222	154,200	154,200	15,250	16,050	70,350	338	10.6	55.6	28.0×10^6
T-222(A)	108,900	91,100	23,950	22,180	52,350	288	23.1	61.1	28.0×10^6
Mo-1/2Ti	165,800	150,400	21,300	14,570	11,600	295	9.3	7.9	45.0×10^6
Cb-1Zr	59,200	59,000	6,650	6,300	29,600	151	14.3	88.4	15.0×10^6
Cb-1Zr(A)	36,300	19,200	13,200	7,050	12,110	99	41.9	91.4	15.0×10^6

Table 10--Mechanical Properties Data at 500°F From Pratt & Whitney Aircraft (CANEL)

Material	Tensile Strength psi	Yield Strength psi	Eng. Strain Energy psi	True Strain Energy psi		DPH Hardness 1.1 Kg.	Elongation %	Area Reduction %	Elastic Modulus psi
304 SS	92,500	56,700	16,150	18,200	37,200	154	30.8	72.9	26.0×10^6
316 SS	72,400	52,300	18,050	17,700	38,000	203	30.4	78.2	26.0×10^6
T-111	101,800	100,800	15,100	10,700	50,900	218	13.8	86.2	27.0×10^6
T-222	133,800	133,800	12,850	12,900	67,800	286	10.9	71.5	27.0×10^6
T-222(A)	92,300	63,400	20,650	33,800	42,200	209	23.6	66.9	27.0×10^6
Mo-1/2Ti	84,100	79,700	10,700	11,000	44,400	207	15.0	75.9	43.0×10^6
Cb-1Zr	54,700	54,700	6,450	5,185	27,700	133	12.7	88.7	14.5×10^6
Cb-1Zr(A)	25,000	11,600	8,100	3,780	7,890	71	35.9	92.2	14.5×10^6

Table 11--Mechanical Properties Data at 70°F From University of Michigan Laboratories

Material	Tensile Strength psi	Yield Strength psi	Engr. Strain Energy psi	True Strain Energy psi		DPH Hardness 1.1 Kg.	Elongation %	Area Reduction %	Elastic Modulus psi
1100-0 Al	12,250	7,600	4,950	4,320	22,600	27	44.5	85.5	10.0×10^6
2024 Al	72,000	57,900	13,300	13,600	31,050	171	20.0	34.5	10.0×10^6
6061 Al	45,300	40,000	25,800	9,840	38,620	127	19.4	56.7	10.0×10^6
Carbon Steel (70°F)	45,300	41,600	18,440	30,530	111,000	193	46.3	76.1	29.0×10^6
Carbon Steel (500°F)	62,510	18,400	19,225	20,900	66,650	125	37.2	63.6	28.0×10^6
Plexiglas	10,445	1,600	320	320	320	9	4.0	0.0	0.4×10^6
Cu	53,400	49,500	3,100	11,800	11,800	133	6.2	19.8	17.0×10^6
Cu-900°F	31,500	9,500	13,900	26,900	26,900	51	51.3	48.5	17.0×10^6
Cu-1500°F	30,700	5,000	6,100	11,800	11,800	41	32.5	33.2	17.0×10^6
Cu-Zn	93,900	82,000	4,700	55,400	55,400	197	5.3	40.7	16.0×10^6
Cu-Zn-850°F	47,600	20,000	28,600	57,000	57,000	71	62.6	60.9	16.0×10^6
Cu-Zn-1400°F	40,400	11,000	15,300	33,000	33,000	48	58.9	51.7	16.0×10^6
Cu-Ni	87,300	77,000	6,100	13,200	13,200	197	4.5	15.4	22.0×10^6
Cu-Ni-1300°F	57,900	20,000	3,100	36,200	36,200	96	34.9	43.5	22.0×10^6
Cu-Ni-1800°F	53,300	18,000	16,300	21,800	21,800	77	34.4	34.4	22.0×10^6
Ni	93,100	82,000	3,200	8,300	8,300	206	3.9	10.2	30.0×10^6
Ni-1100°F	50,500	13,000	18,300	48,300	48,300	67	43.8	51.6	30.0×10^6
Ni-1600°F	48,700	7,000	16,100	40,500	40,500	59	41.8	49.7	30.0×10^6

05031-4-T

Garcia, R.
Comprehensive cavitation damage data for water, mercury, and lead-bismuth alloy including correlations with material and fluid properties, by R. Garcia, F.G.Hammitt, R.E. Nystrom. May 1966

University of Michigan. Dept. of Nuclear Engineering. Laboratory for fluid flow and heat transport phenomena. Tech. Rept. 4

strain as well as reduction of area in computing the breaking stress, while the second value, denoted by TSER, takes into account the "necking" of the specimen in computing the local strain in the failure region, and reduction in area to compute the local true breaking stress. The large discrepancies that exist between these three strain energy values for highly ductile materials indicate the difficulties and uncertainties incurred in using energy as a correlating parameter. If it occurs that the engineering strain energy (ESE) proves to be a better correlating parameter than the true strain energy based on reduction in area (TSER), then this may indicate that brittle rather than ductile failures are typical of cavitation damage.

CHAPTER V

CORRELATIONS OF CAVITATION DATA WITH MECHANICAL AND FLUID PROPERTIES DATA

A. General

To investigate the dependence of cavitation resistance on mechanical material properties and fluid properties, and to obtain a better understanding of the damage mechanisms, it is desirable to subject the damage data and the appropriate mechanical and fluid properties data to a least mean squares fit correlation procedure. For these studies a quite sophisticated least mean squares stepwise regression program[21,22] was utilized. For the first-order interaction form of the program, the problem can be simply stated: it is required to determine the appropriate coefficients and exponents in a predicting equation of the form:

$$Y = C_0 + C_1X_1^{\,a} + C_2X_2^{\,b} + C_3X_3^{\,c} + C_4X_4^{\,d} + \ldots\ldots\ldots + C_nX_n^{\,q} \qquad (1)$$

where C_0, C_1, C_2, C_3, C_4, ..., C_n are constant coefficients; a, b, c, d, ..., q are constant integer or reciprocal integer exponents; X_i are the independent variables, in this case the mechanical properties of the materials and the fluid properties; and Y is the

dependent variable, the average MDP rate. The independent variables are allowed to appear in the predicting equation any number of times, each time raised to a different value of exponent and multiplied by an appropriate coefficient. The general program allows great latitude in the possible exponents. However, that form of the program used here allows any or all of the independent variables to be raised to the following exponents: $\pm 1, \pm 2, \pm 1/2, \pm 3, \pm 1/3$.

A predicting equation of the type of equation (1) would be obtained by allowing only a "first-order interaction" of the possible terms, i.e., terms involving products of the independent variables would not be allowed. The general program, however, also allows the option of a "second-order interaction."

In the present analysis nine mechanical properties (independent variables) were considered, i.e., TS, YS, ESE, TSEE, TSER, H, ELON, RA, and E (symbols as previously explained). In addition one fluid property was included among the independent variables for each of the correlations as a coupling parameter to attempt to account for differences in cavitation resistance of a given material in different fluids. The fluid coupling parameters that were investigated included the ratio of acoustic impedances of test fluid and specimen material (AI), density of fluid (RHO), surface tension (σ), net positive suction head (NPSH), bulk modulus (B), and kinematic viscosity (ν). Hence, a given correlation, there were a total of ten independent variables, and ten possible exponents were allowed for each independent variable. As a result, a total of 100 terms are possible candidates for inclusion in the

predicting equation, plus an additive constant. From a physical point of view, it is desired that a good statistical correlation be obtained with a minimum number of terms so that the predicting equation may hopefully be justifiable on physical grounds. The interested reader is referred to the literature previously cited for further details on the program.

B. Lead-Bismuth Correlations

1. General--The lead-bismuth cavitation data obtained at 500°F and at 1500°F was submitted to the least mean squares regression program to obtain a first-order interaction correlation applicable at both temperatures, and, hence, having the greatest generality allowed by the limited data. The nine mechanical properties (Tables 9, 10, and 11) and one fluid property (Table 8) were taken to be the independent variables with the average MDP rate being the dependent variable. The fluid coupling parameter employed in this case was the ratio of the acoustic impedances of the test fluid and specimen material.* These properties were selected since previous investigators had attempted correlations with them and/or because many of the properties have been involved in hypothesized damage mechanisms.

2. Single Property Correlations--As a first step in the analysis, an attempt was made to correlate the damage data with each

---

*This is one of several quantities that have been chosen as coupling parameters between the fluid and material, and is related to the ratio of reflected to transmitted energy as liquid shock waves or jets impinge on the solid.

mechanical property individually. True strain energy based either on the reduction in area (TSER) or elongation (TSEE) was found quite successful as a single correlating parameter for all of the lead-bismuth data, although, as will be discussed, this was not the case for the other data subsets. The tensile strength, hardness, and engineering strain energy, although having much lower values of coefficient of determination,* are also fairly successful in this regard, while the other mechanical properties are much less so. It is further noted that the average MDP rate is inversely proportional to various powers of true strain energy, engineering strain energy, tensile strength, or hardness in this analysis, as would be expected. The statistically best predicting equation obtained from the single property correlation was:

$$\text{Avg. MDP Rate} = 0.233 + 2.57\times10^{4}(\text{TSER})^{-1} \qquad (2)$$

Coefficient of Determination = 0.986

Average Absolute Per Cent Deviation** = 0.1%

3. Multiple Property Correlations--Further attempts at complete correlations of the experimental data were conducted in which all nine mechanical properties and one fluid property noted previously, each allowed to be raised to ten separate exponents, were possible terms in

---

*The coefficient of determination is a statistical quantity that can be interpreted as the proportion of the total variation in the dependent variable that is explained by the predicting equation. Its values range from 0 (no prediction) to 1.0 (perfect prediction).

**The average absolute per cent deviation is the average of the algebraic deviations existing between individual experimental and predicted values of MDP rate.

the predicting equation. The statistically best predicting equation then obtained was:

$$\text{Avg. MDP Rate} = 0.713 + 3.12\times10^{4}(\text{TSER})^{-1} - 6.55\times10^{4}(\text{TS})^{-1} + 2.97\times10^{21}(\text{E})^{-3} \quad (3)$$

Coefficient of Determination = 0.996

Average Absolute Per Cent Deviation = 0.4%

Note that the true strain energy based on reduction in area (TSER), tensile strength (TS), and elastic modulus (E) all enter the predicting equation in an inverse manner, as was the case with the single property correlations. Also the true strain energy based on reduction in area and the tensile strength, which were both successful as single correlating parameters, are prominent in the multiple property correlating equation.

C. Mercury Correlations

1. Single Property Correlations--True strain energy based on elongation (TSEE) and hardness (H) are quite successful as single correlating parameters for all of the mercury data. Tensile strength, yield strength, and elastic modulus are considerably less successful. The statistically best single-property predicting equation was:

$$\text{Avg. MDP Rate} = 0.338 + 4.90\times10^{7}(\text{TSEE})^{-2} \quad (4)$$

Coefficient of Determination = 0.965

Average Absolute Per Cent Deviation = 8.5%

Note that a different form of strain energy is involved than that used in the best lead-bismuth single property correlation, equation (2), and that the exponent is -2 rather than -1.

2. Multiple Property Correlations--Multiple correlations using all nine mechanical properties and one fluid property were conducted. The statistically best predicting equation was:

$$\text{Avg. MDP Rate} = -0.577 + 1.39\times10^{11}(\text{TSEE})^{-3} + 16.49(\text{H})^{-1/2} \qquad (5)$$

Coefficient of Determination = 0.966

Average Absolute Per Cent Deviation = 10.1%

Note that the true strain energy based on elongation (TSEE) and the hardness (H) enter the predicting equation in an inverse manner, as was the case with the single property correlations. However, the form of strain energy involved differs from that in the lead-bismuth correlation, as does the exponent on this term. These same properties were also successful as single correlating parameters.

D. Water Correlations

1. Single Property Correlations--Hardness, tensile strength, and yield strength were most successful as correlating parameters among the ten properties for the complete set of water data. However, only hardness was reasonably successful from a statistical point of view. For this data set both forms of true strain energy were quite unsuccessful. The statistically best predicting equation obtained in the single property correlations is:

$$\text{Avg. MDP Rate} = -6.023 + 1.30\times10^{4}(H)^{-2} + 53.63(H)^{-1/3} - 6.17\times10^{2}(H)^{-1} - 8.00\times10^{4}(H)^{-3} \quad (6)$$

Coefficient of Determination = 0.946

Average Absolute Per Cent Deviation = 18.7%

The fact that the correlations for water were not as good as for the liquid metals may indicate that other factors not considered in this analysis, e.g., corrosion, may be more important for the water tests.

2. Multiple Property Correlations--When all nine mechanical properties and one fluid property are allowed to enter the predicting equation, the statistically best predicting equation is:

$$\text{Avg. MDP Rate} = -0.068 + 3.07\times10^{8}(TS)^{-2} - 8.32\times10^{-7}(RA)^{3} - 2.03\times10^{3}(H)^{-3} + 1.49\times10^{2}(TS)^{-1/2} \quad (7)$$

Coefficient of Determination = 0.976

Average Absolute Per Cent Deviation = 0.5%

3. Summary--Hardness, tensile strength, and yield strength adequately predict the experimental water data on a single property basis, either for subset one, subsets two and three combined, or the full water data set to which equation (6) applies. In addition the elastic modulus is successful as a single correlating parameter for subset one. These same properties are the most prominent in the ten property water correlations. In fact, generally those properties most successful as single correlating parameters in a given fluid are the most prominent in the ten property correlations.

Whereas energy properties were quite important in the correlation of the data from the tests with high density liquid metals, they are almost completely insignificant in the water tests. On the other hand, the strength properties (including hardness in this category) are predominant in the water tests.

Intuitive arguments can be advanced to show that a correlation would be expected to involve both energy and strength terms. For example, if all cavitation stresses were less than the fatigue limit of a very strong but brittle material, it would not be damaged at all even if the strain energy were zero. On the other hand, a highly ductile material with low strength properties but high strain energy also might not suffer material removal even though considerable surface distortion occurred. It would be expected that the first condition would apply more closely to the water tests (relatively low density fluid) than to the liquid metal tests. Thus these arguments are consistent with the present experimental data.

E. Fluid Coupling Parameters

Thus far, the only property included in the regression analysis that is a function of the fluid has been the ratio of acoustic impedances of the test fluid and specimen material. This quantity was not particularly successful either for the lead-bismuth or mercury data, but was somewhat better for the water data.

It would be desirable to obtain a predicting equation of high statistical accuracy valid for all the lead-bismuth, mercury, and water

data combined. Since the dynamics of bubble growth and collapse are controlled by the physical properties of the fluid, it is necessary to consider the variations in fluid properties for this case. Since the rankings of the materials differed between these various test fluid conditions, it is clear that fluid properties must in some way be considered. This can be done by including one or more suitable fluid coupling parameters among the mechanical properties allowed to enter the predicting equation. The ratio of acoustic impedances is one possible fluid coupling parameter. Other possibilities are fluid density, surface tension, net positive suction head, compressibility or bulk modulus, and kinematic viscosity. The values of each of these properties for the fluid-temperature combinations investigated are listed in Table 8.

F. Comprehensive Lead-Bismuth, Mercury, and Water Correlations

The combined lead-bismuth, mercury, and water data was submitted to the regression program in an attempt to find a single correlation for all the experimental data in terms of mechanical and fluid properties. The mechanical properties considered were those previously used. In addition, each of the six fluid coupling parameters discussed previously was combined separately with the group of nine mechanical properties. Hence six comprehensive correlations were attempted, allowing a total of nine mechanical properties and one fluid property in each. It was hoped that such a procedure would indicate those fluid properties that were most successful as coupling parameters. However, it was found that all

fluid properties considered in this way were fairly successful as coupling parameters. In retrospect this is not surprising since all are smooth functions of each other, and the power series type correlating equation used has sufficient flexibility to accommodate any one of them. For example, with density as fluid coupling parameter, the statistically best predicting equation is:

$$\begin{aligned}\text{Avg. MDP Rate} = {} & 2.44 - 1.62(\text{RHO})^{-1/3} + 4.82\times10^{2}(\text{E})^{-1/3} \\ & + 2.07\times10^{3}(\text{TSEE})^{-1} - 1.99\times10^{13}(\text{E})^{-2} + 4.26\times10^{4}(\text{TSER})^{-1} \\ & - 7.35\times10^{-2}(\text{H})^{1/2} - 5.48\times10^{2}(\text{TSER})^{-1/2} + 2.36\times10^{8}(\text{TS})^{-2}\end{aligned}$$

Coefficient of Determination = 0.969 (8)

Average Absolute Per Cent Deviation = 9.7%

Three of the terms present in the equation involve the true strain energy and two terms are functions of the elastic modulus. The tensile strength and hardness are also present, each indicating that a decrease in damage rate would be expected with increasing tensile strength or hardness. Even though the density term is raised to a negative exponent, increasing density still would result in increased damage, since the whole term has a negative coefficient.

It will be recalled that strain energy, tensile strength, and hardness were the most successful properties in the correlations of lead-bismuth, mercury, and water separately. These mechanical properties along with any of the fluid coupling parameters are also the most prominent in the comprehensive lead-bismuth, mercury, and water correlations.

CHAPTER VI

SUMMARY AND CONCLUSIONS

Ultrasonic-induced cavitation studies have been conducted in lead-bismuth alloy at 500°F and 1500°F, in mercury at 70°F and 500°F, and in water at 70°F for a wide variety of materials, including refractory alloys, steels, brasses, copper, nickel, plastics, etc. The detailed results for the various fluid-material-temperature combinations are listed in the appropriate sections of the report. Various salient features include the following:

a) The tantalum-base alloys, T-111 and T-222, were the most cavitation resistant of the materials tested in lead-bismuth alloy at 500°F and 1500°F, in mercury at 500°F, and in water at 70°F. The stainless steels were the most resistant in mercury at 70°F.

b) As would be expected all materials tested in lead-bismuth sustained greater damage at 1500°F than at 500°F. All materials tested in mercury sustained greater damage at 500°F than at 70°F with the exception of the hot-rolled carbon steel. This can be explained by the superior mechanical properties of this material at the higher temperature.

c) Plexiglas was relatively less cavitation resistant in mercury than in water, and in fact there are numerous substantial

differences in rankings between materials in different fluids at the same temperature. Thus clearly any equation to predict cavitation damage must consider fluid as well as material properties. These observations are consistent with previous venturi test results from this laboratory.

d) Detailed examination of the wetted but non-cavitated parts of the equipment and test specimens indicates that corrosion effects in the absence of cavitation were insignificant in these investigations.

e) For these tests wherein the applied static pressure above vapor pressure was held constant for the different tests, damage rates with mercury were 3 to 20 times greater than for water. The damage noted in lead-bismuth and mercury at 500°F was about the same.

f) In general, the damage rate was constant throughout the tests for the liquid metals and for most of the water investigations. However, in some of the water tests, the damage rate decreased markedly during the test. It is felt that this is a result of the very deep, isolated pitting encountered in these tests. Generally, water tests differed from the liquid metal tests in that quite uniform and relatively fine damage was encountered in the liquid metal tests as opposed to the water tests on the same materials. This may be a result of improper modeling of the fluid flow regime between the two fluids. The test durations were so adjusted that the total accumulative mean depth of

penetration was always less than about ten mils. It is within the range between zero and ten mils MDP (ignoring the very early part of the test below perhaps an MDP of one mil) that the damage rates were substantially constant.

g) Direct comparison of venturi and vibratory results from this laboratory shows that the ranking of materials for cavitation damage are quite similar. The damage rates in the vibratory tests are of the order of 10^3 times those in the venturi, so that corrosive effects are much less important in the vibratory tests.

Computer correlations of the cavitation damage data with applicable mechanical and fluid properties indicate the following important conclusions:

a) There is no single material mechanical property which can be used to correlate the damage, even if coupling parameters to account for fluid property changes are included in the correlation.

b) In general, the best correlations include one or more energy-type mechanical properties, one or more strength-type properties, and one or more fluid coupling parameters if the fluid properties are varied in the data set.

c) The energy-type properties are more predominant in the tests with the high density liquid metals, while the strength-type properties predominate for the water tests. This is consistent with theoretical expectations.

d) No relatively simple single correlating equation applies well to all the data. If sufficient terms are allowed, of course, any degree of statistical fit can be obtained. This lack of a single simple correlating equation may indicate that all important mechanisms in cavitation damage have not been considered. For example, it may not be possible to explain cavitation damage in terms of properties which are determined under semi-static conditions. Final conclusions in this regard must await the obtaining of additional data and more comprehensive correlations.

BIBLIOGRAPHY

1. Royal Society Discussion on Deformation of Solids Due to Liquid Impact, May 27, 1965; London, England.

2. O. Decker, "Cavitation Erosion Experience in Liquid Mercury Lubricated Journal Bearings," First Annual Mercury Symposium, November, 1965, Atomics International, Canoga Park, California, p. 14.

3. A. A. Shoudy and R. J. Allis, "Materials Selection for Fast Reactor Applications," Proc. of Michigan ANS Fast Reactor Topical Meeting, April, 1965, Detroit, Michigan.

4. G. M. Wood, R. S. Kulp, and J. V. Altieri, "Cavitation Damage Investigations in Mixed-Flow Liquid Metal Pumps," Cavitation in Fluid Machinery, ASME, November, 1965, pp. 196-214.

5. P. G. Smith, J. H. DeVan, and A. G. Grindell, "Cavitation Damage to Centrifugal Pump Impellers During Operation with Liquid Metals and Molten Salt at 1050-1400°F," Journal of Basic Engr., Trans. ASME, September, 1963, pp. 329-337.

6. F. G. Hammitt, "Cavitation Damage and Performance Research Facilities," Symposium on Cavitation Research Facilities and Techniques, pp. 175-184, ASME Fluids Engineering Division, May, 1964. See also ORA Technical Report No. 03424-12-T, Department of Nuclear Engineering, The University of Michigan, November, 1963.

7. R. Garcia and F. G. Hammitt, "Ultrasonic-Induced Cavitation Studies," ORA Technical Report No. 05031-1-T, Department of Nuclear Engineering, The University of Michigan, October, 1964.

8. R. Garcia and F. G. Hammitt, "Amplitude Determination of an Ultrasonic Transducer By Means of an Accelerometer Assembly," ORA Internal Report No. 05031-7-I, Department of Nuclear Engineering, The University of Michigan, December, 1965.

9. R. Garcia and F. G. Hammitt, "Ultrasonic-Induced Cavitation in Liquid Metals at 1500°F," Internal Report No. 05031-1-I, Department of Nuclear Engineering, The University of Michigan, February, 1965; also Trans. ANS, Vol. 8, No. 1, pp. 18-19, June, 1965.

10. R. Garcia and F. G. Hammitt, "Ultrasonic-Induced Cavitation in Liquid Metals at 500°F," Internal Report No. 05031-3-I, Department of Nuclear Engineering, The University of Michigan, April, 1965.

11. R. Garcia and F. G. Hammitt, "Ultrasonic-Induced Cavitation Studies in Lead-Bismuth Alloy at Elevated Temperatures," ORA Technical Report No. 05031-2-T, Department of Nuclear Engineering, The University of Michigan, June, 1965.

12. R. Garcia and F. G. Hammitt, "Ultrasonic-Induced Cavitation Studies in Lead-Bismuth Alloy at Elevated Temperatures," to be presented at 1966 National Association of Corrosion Engineers Convention, April, 1966; also available as ORA Internal Report No. 05031-4-I, Department of Nuclear Engineering, The University of Michigan, September, 1965.

13. R. Garcia, R. E. Nystrom, and F. G. Hammitt, "Ultrasonic-Induced Cavitation Studies in Mercury and Water," ORA Technical Report No. 05031-3-T, Department of Nuclear Engineering, The University of Michigan, December, 1965.

14. R. E. Nystrom, "Ultrasonic-Induced Cavitation Study in Mercury at 70°F," M.S.E. Thesis, Department of Nuclear Engineering, The University of Michigan, October, 1965. See also "Ultrasonic-Induced Cavitation Study in Mercury at 70°F," ORA Internal Report No. 05031-6-I, Department of Nuclear Engineering, The University of Michigan, October, 1965.

15. M. S. Plesset and R. E. Devine, "Effect of Exposure Time on Cavitation Damage," ASME Paper No. 65-WA/FE-23; to be published J. Basic Engr., Trans. ASME.

16. Personal communication from Henry P. Leeper, Project Metallurgist, Pratt & Whitney Aircraft (CANEL), to F. G. Hammitt; February 26, 1965, and May 13, 1965.

17. M. John Robinson, "On the Detailed Flow Structure and the Corresponding Damage to Test Specimens in a Cavitating Venturi," Ph.D. Thesis and ORA Technical Report No. 03424-16-T, Department of Nuclear Engineering, The University of Michigan, August, 1965.

18. Curtis A. Harrison, M. John Robinson, Clarence A. Siebert, Frederick G. Hammitt, and Joe Lawrence, "Complete Mechanical Properties Specifications for Materials as Used in Venturi Cavitation Damage Tests," ORA Internal Report No. 03424-29-I, Department of Nuclear Engineering, The University of Michigan, August, 1965.

19. K. K. Shal'nev, "The Energetics Parameter and Scale Effect in Cavitation Erosion," Akademiya nauk SSSR, Izvestiya Otdeleniye teknicheskikh nauk. Mekhanika i mashinomostroyeniye, no. 5, 1961, pp. 3-10.

20. A. Thiruvengadam, "A Unified Theory of Cavitation Damage," Trans. ASME, J. Basic Engr., Vol. 85, 1963, pp. 365-376.

21. Franklin H. Westervelt, "Automatic System Simulation Programming," Ph.D. Thesis, College of Engineering, The University of Michigan, November, 1960.

22. Richard L. Crandall, "The Mathematical and Logical Procedure of the Stepwise Regression Program with Learning," University of Michigan Computing Center Internal Report, 1965.

23. Liquid Metals Handbook, Richard N. Lyon, Editor-in-Chief, Second Edition, June, 1952.

24. International Critical Tables, Compiled by Clarence J. West and Callie Hull, McGraw-Hill Book Company, New York, 1933.